# 1 Influence of Carbon Source and Iron Oxide Minerals on Methane

# 2 Production and Magnetic Mineral Formation in Salt Marsh

# 3 Sediments

10

1112

13 14

15

16

17

18

19

20

2122

2324

25

26

27

28

29

- 4 Kaleigh R. Block<sup>1</sup>, Amy Arbetman<sup>2</sup>, Sarah P. Slotznick<sup>3</sup>, Thomas E. Hanson<sup>1</sup>, George W. Luther III<sup>1</sup>,
- 5 Sunita R. Shah Walter<sup>1</sup>
- 6 <sup>1</sup>School of Marine Science and Policy, University of Delaware, Lewes, DE, USA
- <sup>2</sup>Macalester College, Saint Paul, MN, USA
- 8 <sup>3</sup>Department of Earth Sciences, Dartmouth College, Hanover, NH, USA
- 9 Correspondence to: Sunita R. Shah Walter (suni@udel.edu)

**Abstract.** Salt marshes can emit significant methane to the atmosphere, but these. These emissions are highly variable and, but the cause of this variability is not well-understood. Although methanogenesis should be inhibited by sulfate reduction where sulfate is present due to its thermodynamic unfavorability, methane emissions are not well-predicted by sulfate concentrations. The cause of this variability is unclear, but one and other controls on methane production must be active. One hypothesis is that rather than being outcompeted where sulfate is present, salt marsh methanogens useare fueled by methylated carbon substrates that sulfate reducers do not. In low salinity wetlands, compete for. It has also been shown that crystalline iron minerals have also been found to can facilitate increased methane production in low-salinity wetlands, but this has not been explored in salt marshes. This study documents how different organic carbon sources (monomethylamine and ethanol) and Fe(III) minerals (ferrihydrite, magnetite orand hematite) influence methane production by microbial communities from a polyhaline tidal marsh creek in the Great Marsh Preserve, DE, USA. Carbon source was the majorhad a strong influence on methane production and microbial community composition at by the end of microcosm the incubations. Microcosms amended More methane was produced with monomethylamine produced more methaneamendment than those with ethanol. The, and the highest methane production rates were in microcosms incubations supplied with both monomethylamine and magnetite or hematite amendments. Less methane was produced with monomethylamine and ferrihydrite, a non-conductive iron oxide, and without iron supplementation. This increased methane production in the presence of (semi)conductive iron minerals could indicate that interspecies electron transfer was active in some of our treatments. Instead But instead of the more commonly described syntrophic partners, however, this interaction appears to be between methylotrophic methanogens belonging to Methanococcoides and an unidentified iron reducing bacterial group, possibly Ca. Omnitrophus. Much less measured methane overall—was measured with ethanol amendment—and there was no discernible effect of iron treatment. Aferrihydrite amendments. But in ethanol-amended incubations, a small proportion of anaerobic methane oxidizers was detected in ethanolamended incubations, which suggests eryptie both methane eyeling production and re-oxidation may have occurred, however leading to low measured methane production. Although some iron reduction and Fe<sup>2+</sup> production was observed in all treatments, significant transformation of ferrihydrite to magnetite was observed only with ethanol amendment. If—such microbially-mediated magnetite formation occurs in salt marsh sediment, our observations indicate that the resulting magnetite could enhance methane production by methylotrophic methanogens. This study highlights the importance of methylated compounds such as those released to sediments by *Spartina* grasses to salt marsh methane production as well as the potential importance of iron mineral composition for predicting methane production and iron reduction rates.

# 1 Introduction

30

3132

33

34

35

36

37

38

39

40

41

42

43

44

45

46 47

48 49

50

5152

53

54

55

56

57

58

59

60

61

Wetlands are the primary natural source of methane emissions to the atmosphere (Saunois et al., 2016; Zhang et al., 2017). However, only a fraction of these emissions is expected to come from high-salinity tidal wetlands such as salt marshes due to the influx of oxygen and sulfate during regular inundation (Bartlett et al., 1987; Hartman et al., 2024; Holmquist et al., 2023; Poffenbarger et al., 2011). According to the textbook paradigm, this is because thermodynamic considerations determine the dominance of microbial metabolisms. Organic carbon degraders are expected to follow the redox ladder, sequentially depleting oxygen, nitrate, manganese and iron oxidesoxide minerals, and sulfate before methanogenesis is favored (Jørgensen, 2006; Jørgensen and Kasten, 2006; Sundby, 2006). In salt marshes, oxygen is often depleted within millimeters of the sediment surface and sulfate reduction is responsible for a large fraction of organic carbon remineralization (Howarth, 1984; Howarth and Giblin, 1983; Howarth and Teal, 1979), as well as the oxidation of methane (Krause and Treude, 2021; Segarra et al., 2013). However, in more oxygenated marsh regions like creek banks and bioturbated zones where pore waters are more efficiently flushed by the tides-and there is more influx of oxygen, iron reduction can be the dominant microbial metabolism (Antler et al., 2019; Gribsholt et al., 2003; Kostka et al., 2002a, b.; Krause et al., 2025). Iron oxides may also fuel anaerobic methane oxidation in salt marshes (Krause and Treude, 2021; Liu et al., 2025; Segarra et al., 2013). HighSalt marsh sediments can also have high iron concentrations have been reported in salt marsh sediments with seasonally-fluctuating mineralogy (Kostka et al., 2002a, b; Kostka and Luther, 1994, 1995; Taillefert et al., 2007). Based on energy yield, the presence of measurable iron oxide minerals and sulfate should inhibit methanogenesis as well as facilitate the anaerobic oxidation of methane produced at deeper depths before it is released to marsh creeks and the atmosphere. At the ecosystem scale, methane emissions data from wetlands do follow a general decreasing trend with increasing sulfate concentrations (Al-Haj and Fulweiler, 2020; Chmura et al., 2011; Hartman et al., 2024; Poffenbarger et al., 2011), but significant variability in methane emissions across salinity gradients has also been reported, indicating the importance of other controls (Al-Haj and Fulweiler, 2020; Bridgham et al., 2006; Chmura et al., 2011; Hartman et al., 2024; Rosentreter et al., 2021). In the mid-Atlantic region of the U.S., high concentrations of methane and indications of active methanogenesis were found to coexist with sulfate reduction in marsh sediments (Seyfferth et al., 2020). This finding indicates thermodynamics does not entirely predict the activity of microbial metabolisms and biogeochemical processes in salt marshes. Methanogens

have been shown to co-exist with sulfate reducers, although with lower activity (Sela-Adler et al., 2017; Senior et al., 1982). They have also been shown to circumvent the redox ladder through utilization of organic substrates that are not as available to sulfate-reducing bacteria such as methylated compounds (Buckley et al., 2008; Oremland et al., 1982; Parkes et al., 2012a; Winfrey and Ward, 1983; Yuan et al., 2019). In the eastern U.S., the low marsh is dominated by the native marsh grass, Spartina alterniflora, which releases trimethylamine at depth through root exudates and root degradation (Wang and Lee, 1994a). Trimethylamine, dimethylamine and monomethylamine have all been detected in the pore waters and sediments of salt marshes (Fitzsimons et al., 1997); Parkes et al., 2012b; Summons et al., 1998; Wang and Lee, 1994b). As sulfate-reducing bacteria deare not known to utilize methylamines, (Mausz and Chen, 2019), this supply of carbon substrate from S. alterniflora allows methanogenesis to proceed simultaneously with sulfate reduction (Seyfferth et al., 2020; Yuan et al., 2014, 2019). Methanogens can also skip rungs of the redox ladder by participation in syntrophic relationships with iron-reducing bacteria (Cruz Viggi et al., 2014; Kato et al., 2012; Rotaru et al., 2014a, 2021; Xu et al., 2019; Zhuang et al., 2019). Although this has not yet been observed in salt marsh microbial communities, methanogens can obtain their reducing equivalents through interspecies electron transfer (IET) facilitated by conductive iron minerals (Lovley, 2017a, b; Rotaru et al., 2021). Although the majority of iron in shallow marsh sediments undergoes a seasonal alternation between amorphous Fe(III) minerals and iron sulfides at shallow depths (Koretsky et al., 2003; Kostka and Luther, 1994), crystalline Fe(III) minerals with (semi)conductive properties that could facilitate IET have been shown to persist year-round, even at anoxic and sulfidic depths (Kostka and Luther, 1994, 1995; Taillefert et al., 2007). It has also been shown that ferrihydrite, an amorphous Fe(III) mineral, can be converted to the secondary conductive mineral magnetite over time in anoxic incubations of microbial communities from rice paddy soils, eventually enhancing methane production through IET (Tang et al., 2016; Zhuang et al., 2015, 2019). Although they have not been as extensively studied as sulfate reducers, iron-reducing bacteria have been reported in salt marsh sediments (Hyun et al., 2007; Koretsky et al., 2003, 2005; Lowe et al., 2000). These populations have the potential to cooperate with methanogens through IET or to outcompete them and transform Fe(III) minerals into aqueous Fe<sup>2+</sup>, mixed-valent minerals like magnetite, or Fe(II) minerals like pyrite. Salt marshes, with their naturally variable redox conditions, have also been found to host greigite-producing magnetotactic bacteria, often in sediments at the transition between oxic and anoxic conditions (Bazylinski et al., 1991; Blakemore, 1975; Demitrack, 1985; Simmons and Edwards, 2007a, b; Sparks et al., 1989). And both magnetite- and greigite-producing magnetotactic bacteria have been found in salt ponds neighboring salt pondsmarshes (Simmons et al., 2004; Simmons and Edwards, 2007b). In this study, we investigate how specific carbon sources and Fe(III) minerals influence the production of methane and magnetic minerals in anoxic, sulfate-free incubations of marsh creek sediments from a polyhaline salt marsh in the mid-Atlantic region of the eastern U.S. We studied non-vegetated marsh creek sediments adjacent to a marsh platform dominated by S. alterniflora to avoid the multiple and confounding influences of marsh grass stems and roots on redox conditions and methane emissions (Määttä and Malhotra, 2024). We investigated the effect of adding organic carbon substrates for methylotrophic and acetoclastic methanogenesis combined with iron minerals that supply Fe(III) with a range of reactivity and electrical

62

63

6465

66 67

68

69

70

71

72

73

74

75

76

77

78

79

80

81

82

83

84

85

8687

88

89

90

91

92

93

94 95

conductivity. Here we compare methane production from monomethylamine (MMA), which represents methylated

methanogenic substrates (Krause and Treude, 2021), to methane production from ethanol (EtOH), which is oxidized to acetate through fermentative pathways (Schink, 1997) and which has been used in many studies investigating the potential for magnetite and hematite to promote electric syntrophy between methanogens and bacteria in soil and sediment enrichments (Kato et al., 2012; Rotaru et al., 2019, 2018, 2019). MMA and EtOH amendments were combined with additions of magnetite, hematite, and ferrihydrite to determine the influence of these iron minerals on methane production and iron reduction by salt marsh microbial communities.

## 2 Materials and Methods

## 2.1 Study Site Description and Sediment Sampling

Sediments for this study were sampled from the Great Marsh Preserve in Lewes, DE, USA. In this location, low marsh is dominated by the marsh grass *S. alterniflora* and it is dissected by a grid of marsh creeks originally dug as mosquito ditches in the 1930's but left to return to natural conditions by the 1970's. The marsh creeks and low marsh platform regularly experience inundation at high tide with water from the lower Delaware Bay via the Roosevelt Inlet and Canary Creek. High tide salinity averages 30 PSU during the month of June (2016–2020 average; Delaware Water Quality Portal Station BR40, 2024), and the tidal amplitude averages 1.2 meters (Dewitt and Daiber, 1973; Guider et al., 2024). Sediments for our study were collected by push core from a mud flat adjacent to the low marsh platform within a marsh creek (38.78926° N, 75.16968° W) while it was covered by shallow water at low tide. The mud flat was selected to avoid living *S. alterniflora* stems and roots. Two sediment cores of 8.5 cm diameter and 22.5 cm length were taken on June 29, 2023. They were processed for geochemistry within five hours of collection.

## 2.2 Downcore Profiling of Redox Conditions

Before the sediment core was extruded in the laboratory, cyclic voltammetry (CV) was used to determine concentrations of dissolved O<sub>2</sub>, ΣH<sub>2</sub>S, ΣS<sup>2-</sup>, Fe<sup>2+</sup>, Fe<sup>3+</sup>, and FeS<sub>aq</sub> molecular clusters on the intact core as well as qualitative concentrations of solid Fe(III) nanoparticles, and organic-Fe(III) aggregates. CV measurements were made with a three-electrode system composed of a solid-state gold amalgam (Au/Hg) working microelectrode encased in glass, a silver-silver chloride (Ag/AgCl) reference electrode and 0.5 mm platinum wire counter electrode (Brendel and Luther, 1995). Electrodes were coupled to a model DLK-60 electrochemical analyzer (Analytical Instrument Systems Inc, Flemington, NJ, USA). The reference and counter electrodes were secured to the core barrel such that they were suspended in marsh creek water, approximately 2 cm of which was retained above the sediment in the core barrel. The working electrode was lowered into the core at fine vertical resolution by a micromanipulator (Luther et al., 2008). Concentrations of ΣS<sup>2-</sup> and O<sub>2</sub> were calculated from current using published parameters (Luther et al., 2008; Waite et al., 2006). Between the sediment-water interface and 0.35 cm depth, measurements were taken every 0.05 cm. Below 0.35 cm, measurements were taken every 0.1 cm until a depth of 1.2 cm.

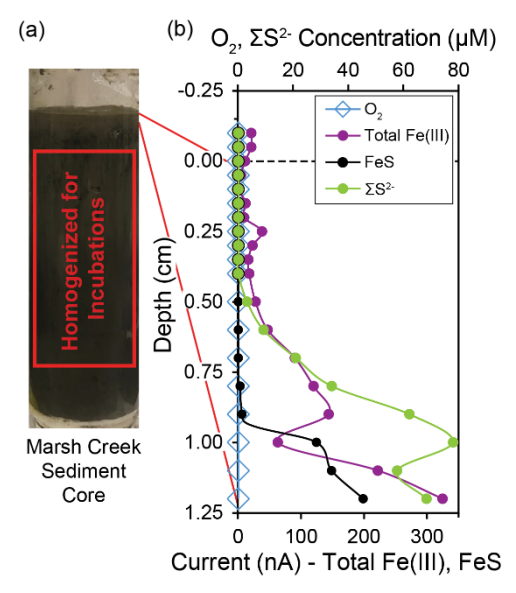
Since the redox transitions were detected at shallower depths, CV measurements were discontinued at a depth of 1.2 cm. All scans were made in triplicate.

## 2.3 Ferrihydrite Synthesis

Ferrihydrite was synthesized following the methods of (Smith et al., 2012). Ferric nitrate nonahydrate (20.25 g) and ammonium bicarbonate (11.91 g) were ground together with a mortar and pestle. The product of this reaction was dried overnight, rinsed the following day via vacuum filtration with small aliquots of deionized water, and dried again overnight. The final product was ground again with a mortar and pestle and used for ferrihydrite amendments in incubations.

## 2.4 Incubations

Although we observed a redox transition at ~0.5 cm, sediments were unconsolidated at this depth. To avoid mixing soluble oxidants in during core sectioning(e.g., oxygen, nitrate, sulfate) from shallower depths into sediments used for incubations from below the redox transition, the top 2.5 cm of the core was conservatively discarded following CV measurements (Fig 1a). Sediments between 2.5 cm to 16.5 cm depth were provided sufficient sediment volume for our incubations and this interval of sediment was extruded and homogenized in a sealed plastic 2.7 mil thickness, low-density polyethylene (LDPE) zip-top bag. The small amount of dead plant material within the core was removed by hand picking during extrusion and transfer to the bag. Homogenized sediments were refrigerated at 4° C for ~16 hours prior to mixing sediments into a slurry and assembling the incubation bottles. Anaerobic incubations were performed in 125 mL serum bottles containing 50 mL of slurry The slurry was made up of 1:3 v/v homogenized marsh sediment and artificial sulfate-free seawater under a N2/CO2 (80/20) headspace. Sulfate was not included in our artificial seawater to disadvantage sulfate reduction in favor of other microbial metabolisms



and allow investigation of controls on methane production other than competition with sulfate-reducing bacteria. Artificial sulfate-free seawater contained 26.4 g NaCl, 11.2 g MgCl<sub>2</sub>·6H<sub>2</sub>O, 1.5 g CaCl<sub>2</sub>·2H<sub>2</sub>O and 0.7 g KCl per liter (Aromokeye et al., 2018) as well as 1 mM of a an iron-free trace metal solution modified from DSMZ Trace Element Solution SL-10 (Koblitz et al., 2023): 70.0 mg ZnCl<sub>2</sub>, 100 mg MnCl<sub>2</sub>·4H<sub>2</sub>O, 6 mg H<sub>3</sub>BO<sub>3</sub>, 190 mg CoCl<sub>2</sub>·6H<sub>2</sub>O, 2 mg CuCl<sub>2</sub>·2H<sub>2</sub>O, 24 mg NiCl<sub>2</sub>·6H<sub>2</sub>O, and 36 mg Na<sub>2</sub>MoO<sub>4</sub>·2H<sub>2</sub>O per liter. Anaerobic incubations were performed in 125 mL serum bottles containing 50 mL of

slurry and 75 mL of headspace. The headspace was purged of O<sub>2</sub> by flushing for 2 minutes with N<sub>2</sub>/CO<sub>2</sub> (80/20) prior to sealing the bottles with an N<sub>2</sub>/CO<sub>2</sub> (80/20) headspace. Incubations were supplemented with 20 mM organic carbon, either ethanol (EtOH) or monomethylamine hydrochloride (MMA). Incubations were also supplemented with 20 mM powdered iron minerals, either synthesized ferrihydrite, magnetite, or hematite, or no iron. Powdered magnetite was purchased from Sigma-Aldrich (St. Louis, MO, USA), and powdered hematite was purchased from Strem Chemicals Inc. (Newburyport, MA, USA). In total, 24 bottles were prepared with the following treatment groups in triplicate: EtOH + no iron, EtOH + ferrihydrite, EtOH + magnetite, EtOH + hematite, MMA + no iron, MMA + ferrihydrite, Figure 1: Redox conditions and sampling depths in the marsh-creek sediment core. (a) Photo of 22.5 cm sediment core before extrusion with interval of sediment used for incubations highlighted. (b) Microelectrode profiles of oxygen, iron and sulfur species with depth in the sediment core as measured by cyclic voltammetry. Total Fe(III) includes Fe(III)(aq), Fe(III)(s) nanoparticles of multiple sizes, and Fe(III) with organic ligands. Total Fe(III) and FeS are plotted with relative units. Traces of FeS were detected beginning at 0.5 cm. O2, Fe3+, and IIS-were not detected in the sediment core or overlying water. The dashed line at 0 cm represents the sediment water interface and negative depths represent height in overlying water.

MMA + magnetite and MMA + hematite. Incubations were maintained at 30° C under static conditions in the dark over the course of the experiment. At the end of the incubations, slurries were homogenized and subsamples were taken for DNA extraction. Sediment was then recovered by centrifugation of the slurries. The supernatant was discarded and sediments were frozen at 80° C under an argon headspace until further processing for magnetic measurements, for 34 days.

## 2.5 Methane and Ferrous Iron Measurements

Headspace methane concentrations were measured twice weekly by gas chromatography with a flame-ionization detector (Agilent 7890B, Wilmington, DE, USA). Methane was separated isothermally on a HP-Plot Q column (Agilent, 30 m x 0.530 μm inner diameter, 40 μm film thickness). Headspace samples were manually injected with a gastight syringe in split mode with split ratio of 5:1. The injector temperature was 250° C, oven temperature was 60° C and detector temperature was 250° C. Methane peaks were integrated using Agilent ChemStation Data Analysis software version F.01.03. A parallel set of 125 mL serum bottles were prepared as methane standards with the same ratio of distilled water to headspace as incubation bottles to account for dissolved methane. The headspace of the standard bottles was filled with 80/20 N<sub>2</sub>/CO<sub>2</sub> and varying amounts of methane. Six standards with total methane concentrations ranging from 0.004 to 0.4 mmol were injected with each set of headspace methane measurements to obtain calibration curves. Methane concentrations and calculated methane production rates in incubations (Figs. 2, 3) were determined from a calibration curve of equilibrated standards and the ideal gas law. Measurements of dissolved ferrous iron were made twice weekly. Ferrous iron was quantified utilizing the ferrozine assay method developed by (Stookey, 1970). From each incubation, 0.5 mL of slurry was sampled from the bottles, filtered at 0.45 μm and stabilized in ferrozine solution. Absorbance at 562 nm was measured with a HP-8452A Diode Array spectrophotometer (Hewlett-Packard/Olis Inc., Athens, GA, USA).

#### 2.6 DNA extraction, PCR, quantification, and sequencing

At the end of the incubation period, one soluries were homogenized and subsamples were taken for DNA extraction. One bottle was selected at random from each treatment group for amplicon sequencing. DNA was extracted from the slurry using the DNeasy PowerSoil Pro Kit (QIAGEN, Germantown, MD, USA). Concentrations of DNA were quantified with a Qubit BR

DNA assay (Invitrogen, Eugene, OR, USA) using a DeNovix DS-11 fluorometer (Wilmington, DE, USA). For all extractions, 185 the total amount of DNA recovered was ≥ 6 ng. Amplification of extracted DNA was performed with a modified two-step 186 187 barcoding method (Herbold et al., 2015; Tadley et al., 2023). Amplicons of the V4 region of the 16S rRNA gene were produced 188 with the primers 515F (Parada et al., 2016) and 806R (Apprill et al., 2015) modified with the head sequence: 5'-GCTATGCGCGAGCTGC-3' (Herbold et al., 2015). The second PCR barcoding primer was paired to the head sequence. 189 190 Each PCR reaction contained 1.0 μM forward and reverse primers in Invitrogen SuperFi Master Mix (Thermo Fisher Scientific, Waltham, MA, USA) with denaturation at 95° C for 30 seconds, annealing at 60° C for 30 seconds and extension at 72° C for 191 192 60 seconds for a total of 30 cycles in the first PCR and 5 cycles for the second PCR. During the first PCR, reactions were 193 completed in triplicate and PCR products were screened by gel electrophoresis. The barcoded amplicons were purified with 194 sparQ PureMag beads (QuantaBio, Beverly, MA, USA). Sequencing on an Illumina MiSeq platform (MiSeq Reagent Kit v2, 195 2 x 250 bp, San Diego, CA, USA) was performed at the University of Delaware Sequencing and Genotyping Center. 196 Amplicon sequences were analyzed as described by (Tadley et al. (... 2023). Sequences were sequentially processed with Python (3.10.10) and QIIME2 (2021.2; Bolyen et al., 2019) for demultiplexing as described by Herbold et al. (2015). Amplicon 197 198 sequence variants were identified with DADA2 (per pipeline tutorial v1.16, DADA2 v1.21.0; Callahan et al., 2016) with 199 quality trimming at Q30 per sample as determined by FASTX-Toolkit (v0.0.14; Gordon et al., 2010). Taxonomy for all 200 amplicons was assigned with the RDP classifier using a classifier based on the Silva 138 SSU Ref NR 99 database for 16S 201 rRNA (Robeson et al., 2021). Relative abundance plots for taxa were generated in R using the FeatureTable package (version 0.0.11; Moore, 2020). Cluster dendrograms were generated using the pvclust R package (version 2.2.0; Suzuki et al., 2019) 202 203 after double square root transformation to reduce artifacts from the large amount of ASVs that were individually relatively rare. Indicator analyses were completed using the indicspecies package in R (version 1.7.15; De Cáceres et al., 2010, 2012). 204

## 2.7 Magnetic measurements

205

206

207

208

209

210

211

212

213214

215

216

217

Magnetic mineral measurements were made on pure iron oxide minerals used for amendments in incubations, on initial homogenized sediment prior to incubation before addition of iron amendments, and on sediments recovered at the end of the incubations. For sediments recovered after incubations, one At the end of incubations, and following subsampling for DNA, sediment was recovered from slurries by centrifugation. The supernatant was discarded and sediments were frozen at -80° C under an argon headspace until they were processed further. One bottle from the three replicates was selected at random from each treatment for magnetic measurements. Initial and post-incubation sediments were freeze-dried, pulverized with a mortar and pestle and stored under an argon headspace until further processing the next step of preparation. Powdered minerals and sediments were prepared for analysis by packing into gel capsules with quartz wool in an anaerobic glovebox. Magnetic analysis of minerals and sediments was performed on a Lakeshore 8604 Vibrating Sample Magnetometer (VSM). The VSM was used to obtain hysteresis loops and direct current demagnetization at room temperature. Data from these VSM measurements are used to characterize and quantify the mineralogy, abundance, and grain size of magnetic minerals. (Fig. 4). Hysteresis loops were slope-corrected to remove antiferromagnetic, paramagnetic, and diamagnetic contributions and then

saturation magnetization and coercivity were extracted for the ferromagnetic (sensu lato) components (Jackson and Solheid,

2010). The direct current demagnetization data was used to find the coercivity of remanence. Its first derivative also produced

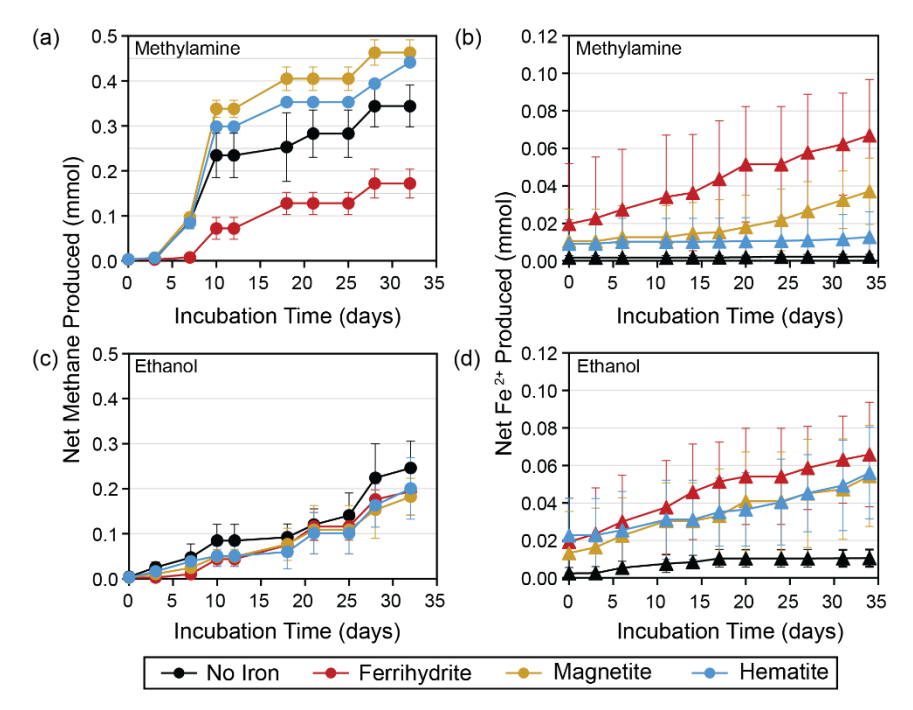
coercivity spectra, which were deconvolved using the Max Unmix software program (Maxbauer et al., 2016).

## 3 Results

## 3.1 Concentrations of Redox-Active Species by Cyclic Voltammetry

NoBy the time cyclic voltammetry measurements were made, two hours after the core was collected, no dissolved oxygen was detected throughout the core, even at the sediment-water interface, by the time cyclic voltammetry measurements were taken two hours after the core was collected. However, at each measured depth within the sediment, at least one form of Fe(III) was detected throughout the measured interval of the sediment core, the upper 1.2 cm (Figs. 1b, A1). We detected multiple forms of Fe(III) asincluding organic-Fe(III) aggregates and nanoparticles of different sizes (Fig A1). The Fe(III) response generally shifted to more negative applied potential with depth in the core (Fig. A1) suggesting increasingly larger particles and an aging process (Taillefert et al., 2000). Reduced sulfur species (ΣS<sup>2-</sup>) were detected at 0.5 cm and deeper in the core, increasing in concentration to 78 μM at 1.0 cm. FeS was also detected at 0.5 cm depth and increased in concentration until the end of measurements at 1.2 cm (Fig. 1b). Although free or unbound ΣH<sub>2</sub>S and Fe<sup>2+</sup> were not detected themselves, rapid reduction of Fe(III) nanoparticles and formation of FeS has been demonstrated in the Marsh creek sediments themselves therefore supplied our incubations with iron and reduced sulfur in multiple forms and multiple oxidation states.

Figure 2: (a) Net methane and (b) Fe<sup>2+</sup> produced with methylamine amendments and all iron treatments averaged over three replicates. Similar plots for (e) net methane and (d) Fe<sup>2+</sup> produced with ethanol amendments are also averaged over three replicates. Error bars represent the standard deviation from the replicates' average value.



presence of inorganic sulfide (Taillefert et al., 2000). It is therefore likely that sulfide produced through microbial activity was rapidly converted to FeS at shallow sediment depths. The presence of free ΣH<sub>2</sub>S at deeper depths than FeS<sub>(sq)</sub> has been previously reported in marsh creeks and estuarine sediments (Taillefert et al., 2002a, b). It is therefore likely that free ΣH<sub>2</sub>S was also present in our core at deeper depths than we measured. Marsh creek sediments themselves therefore supplied microcosms with iron and reduced sulfur in multiple forms and multiple oxidation states.

## 3.2 Methane Production and Iron Reduction in Incubations

Methane production was observed in all microcosm incubations. incubation bottles. The most methane was, along with the highest and most consistent methane production rates, were produced in bottles amended with MMA and magnetite or hematite followed by MMA without iron amendment (Figs. 2a, 3a,b). All other treatments produced similar quantities of methane (Fig. 2a,c). The highest production rates overall were observed within the first 10 days followed by lower sporadic pulses (Fig. 3). In addition to producing the most methane, MMA + magnetite and MMA + hematite bottles displayed the highest and most consistent methane production rates, particularly early in the incubations (Fig. 3a,b). MMA bottles with MMA + ferrihydrite took longer to ramp up methane production compared to the MMA with other iron treatments or no iron (Figs. 2a, 3c). On average, MMA + no iron bottles produced more methane than EtOH + no iron (Fig. 2a,c), although however, methane production in no-iron incubations was more variable than it was with an iron amendment for both MMA and EtOH treatments with no added iron (Fig. 3d).-

With the exception of MMA + ferrihydrite, bottles amended with EtOH produced less methane than MMA-amended bottles

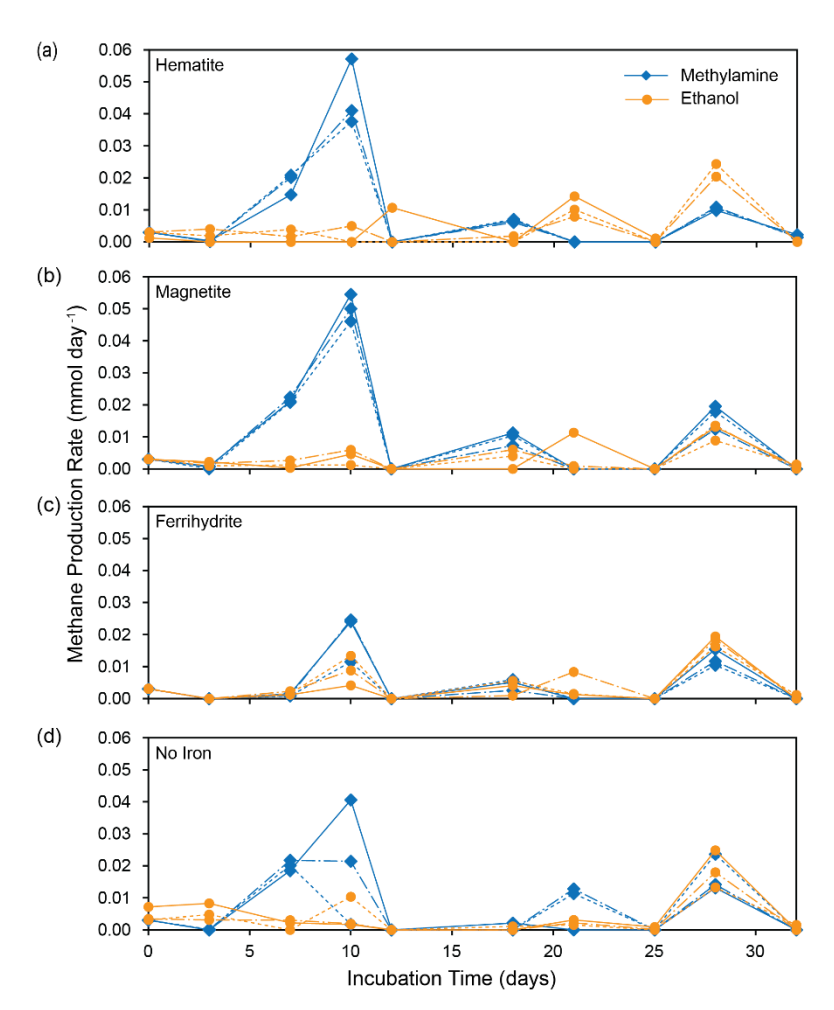


Figure 3: Methane production rates for each incubation bottle shown for MMA incubations (blue) and EtOH incubations (orange) separated by iron treatment.

with the same iron treatment, in all cases except with ferrihydrite amendment, in which methane production was comparable.

There was also no significant difference between EtOH incubations with different iron treatments

(Fig. 2c). In all EtOH-amended incubations, the highest methane production rates were observed as sporadic pulses late in the incubation period (Fig. 3). However, after the first 10 days, the trajectory of methane production was approximately the same regardless of organic carbon or iron treatment. For example, all treatments had a moderate peak in methane production on day 2528 (Fig. 3). This similarity suggests that by the final two weeks of the incubation period, methane production rates were no longer related to the initial organic carbon amendments.

As  $Fe^{2+}$  concentrations reflect both production by microbial iron reduction and loss from iron mineral formation, they are less sensitive as a tracer of microbial activity than methane concentrations. We therefore treat  $Fe^{2+}$  concentrations as an indicator of iron reduction kinetics following the approach of previous studies (Aromokeye et al., 2018). The most net  $Fe^{2+}$  production occurred in bottles with ferrihydrite amendments regardless of organic carbon treatment (Fig. 2a,c), suggesting ferrihydrite

yielded the highest iron reduction rates. In EtOH bottles, magnetite and hematite yielded almost as much  $Fe^{2+}$  as ferrihydrite with a similar production rate in the first 10 days (Fig. 2d). With the MMA amendment, on the other hand, iron reduction was mineral-specific. Incubations with magnetite did not ramp up  $Fe^{2+}$  production until the final two weeks, and MMA + hematite incubations did not show evidence of significant iron reduction at any point during the incubation period (Fig. 2b).

## 3.3 Magnetic Mineral Formation

269

270

271

272

273

274

275

276

277

278

279

280

281282

283

284

285

286287

288

289

290

291

292

293

294

295

296

297

298 299

300

301

In bottles amended with EtOH and ferrihydrite, a progressive shift from reddish ferrihydrite to a dark gray magnetic mineral was observed over the course of the incubation (Fig. C1). To further characterize magnetic mineral formation, magnetic measurements were made. However, since such extensive transformation of ferrihydrite was not anticipated, we did not preserve subsamples of initial slurry with iron amendments for magnetic mineral characterization. Instead, initial sediments without iron amendments and each powdered iron mineral were characterized individually and used to contextualize magnetic measurements made on sediments recovered at the end of the incubations. Ferromagnetic minerals were identified and further characterized by their remanent coercivities, and saturation magnetization was used to measure ferromagnetic mineral abundance. Magnetite-amended incubations are not discussed further in the main text because the amendment itself overwhelmed any detectable change in magnetic minerals that may have occurred during the incubation (Fig. C2, Table C1). In initial homogenized sediments, a small but measurable saturation magnetization indicated the presence of magnetic minerals (Fig. 4a). This concentration was typical of magnetic mineral concentrations measured in sediments across a wide range of conditions (Kreisler and Slotznick, in revision). The presence of a ferromagnetic mineral with mid-coercivity (B<sub>cr</sub> = 39 mT), interpreted to be magnetite, as well as a minor high coercivity component, interpreted to be hematite, were both detected (Fig. 4c). At the end of the incubation period, the saturation magnetization of sediments recovered from the iron-free treatments looked similar to initial measurements. Small increases in most other treatments are hard to deconvolute from the addition of ferromagnetic mineral amendments (Fig. 4a, hematite incubations described further in Appendix C). The iron-free, hematite, and MMA + ferrihydrite treatments all had remanent coercivities and coercivity spectra similar to the initial sediment slurry (Figs. 4b, C2). However, the EtOH + ferrihydrite treatment showed a large increase in saturation magnetization (Fig. 4a). This signal could not have resulted simply from the addition of ferrihydrite to initial sediments because ferrihydrite itself is antiferromagnetic to weakly ferromagnetic. Although the synthesized ferrihydrite analyzed contained a small ferromagnetic component, its saturation magnetization was similar to that of the hematite standard and an amended bottle with no further mineralogical changes would be comparable. This indicates that the EtOH + ferrihydrite treatment was the only one that produced significant quantities of measurable ferromagnetic minerals. A large decrease in bulk remanent coercivity was noted with EtOH + ferrihydrite treatment as well (Fig. 4b); coercivity spectra show that the predominant phase produced in the EtOH + ferrihydrite treatment is within the range for magnetite (B<sub>cr</sub>~\_9 mT) (Fig. 4d)—(; Peters and Dekkers, 2003). Coercivity is not a definitive mineral identifier and other ferromagnetic minerals have overlapping coercivity ranges, specifically pyrrhotite and greigite, but the low abundance of sulfide suggests it is not either of these phases. Notably, the ferromagnetic mineral produced

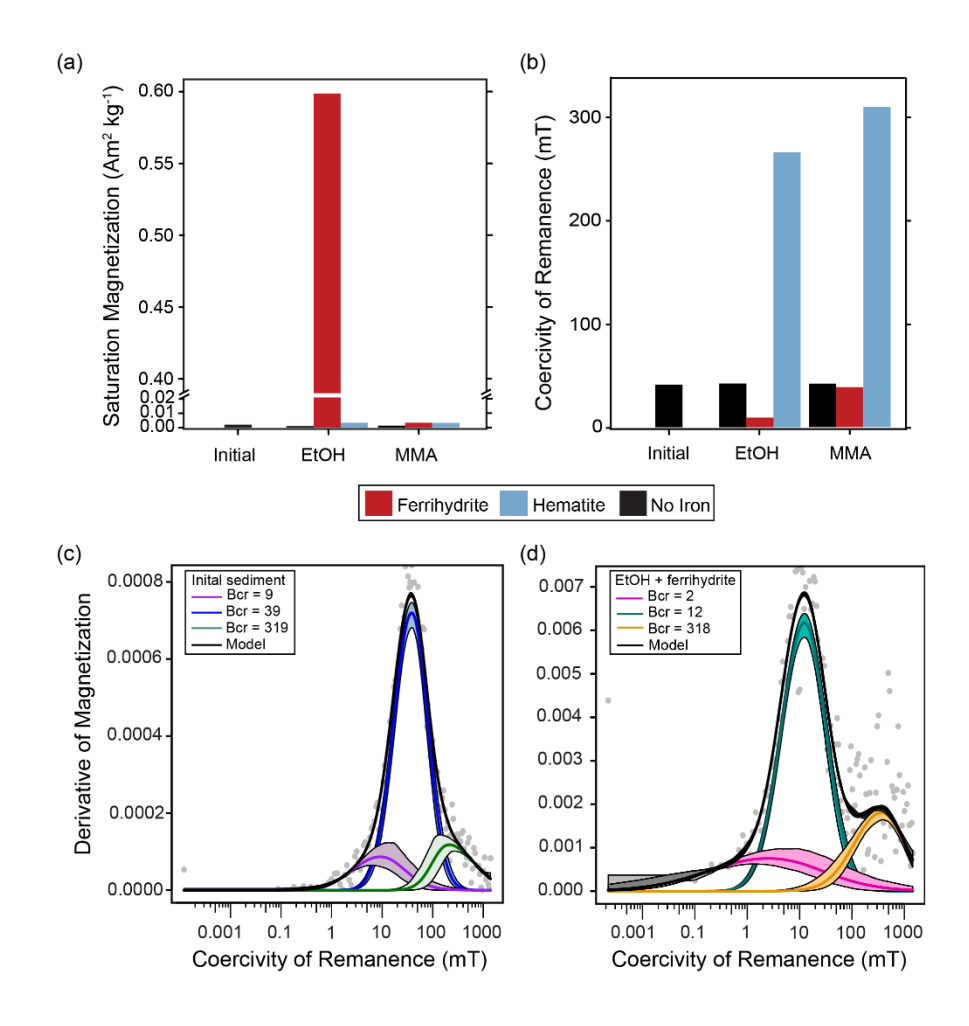
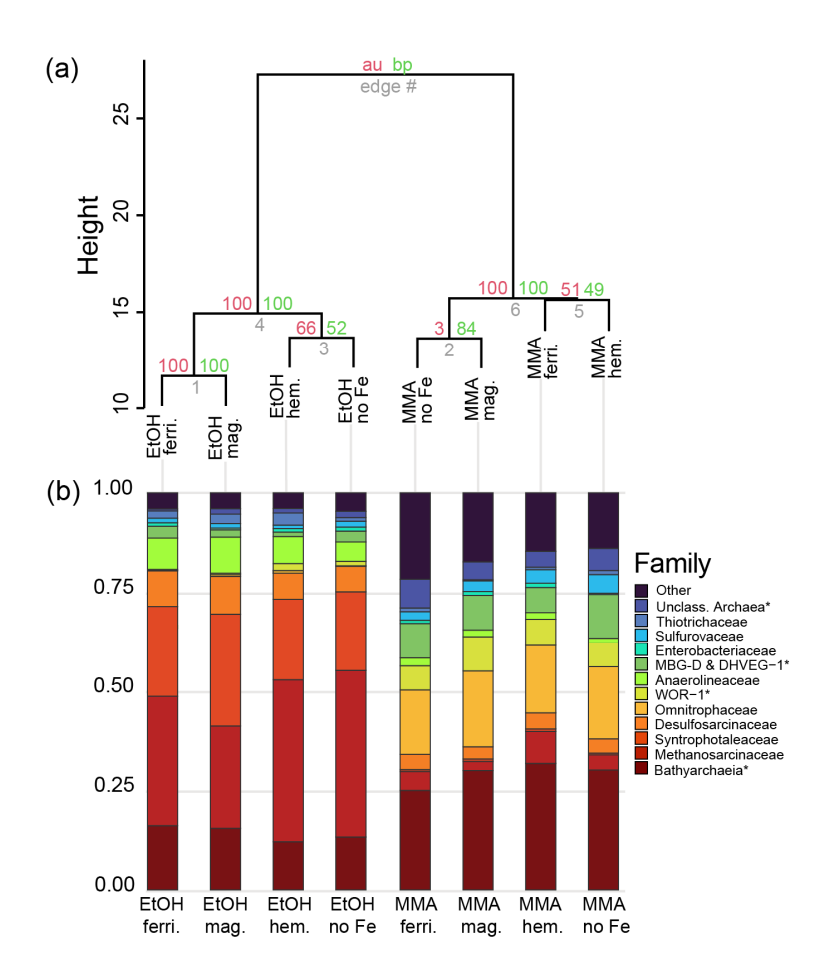


Figure 4: Ferromagnetic mineral measurements of initial homogenized sediment used in all incubations and sediment recovered from all amended incubations at the end of the incubation period. (a) Abundance of ferromagnetic minerals as indicated by saturation magnetization (Ms, Am² kg¹ of dried sediment sample). (b) Mineral identification summarized by coercivity of remanence (Bcr; mT). Examples of MAX UnMix data for (c) initial sediment with no iron mineral amendment and (d) EtOH + ferrihydrite sediment at the end of the incubation period. Data from sediments amended with magnetite are not shown as magnetite amendment itself overwhelmed any signals of magnetite formation or loss.

during EtOH + ferrihydrite incubations has a lower coercivity than the magnetite in initial sediments (Fig. 4c,d). It is therefore likely to be a more fine grained magnetite than is found natively in the marsh sediments. In addition to this predominant mid-coercivity phase, there appears to be a slight increase in abundance of high-coercivity phases as well ( $B_{cr} = 318$ ), interpreted as hematite. A similar change is not seen in the MMA + ferrihydrite treatment, suggesting this is not simply due to abiotic aging of ferrihydrite, but could be related to microbial iron-oxidation of fine grained magnetite instead of *de novo* production.



# 3.4 Microbial Community Composition

Microbial community composition at the end of the incubations from 16S rRNA sequence data is shown in Fig. 5 for families that represented > 5% of total sequences. To facilitate more detailed comparisons, archaeal and bacterial community composition is also shown at the taxonomic level of genus in Fig. 6 for genera representing > 5% of sequences from each domain. Hierarchical clustering of 16S rRNA sequences from the end of microcosm-incubations (Fig. 5a) showed a clear pattern that was aligned with carbon substrate. The same pattern was observed when just bacterial or archaeal sequences were used (Fig.

Figure 5: Microbial community composition from 16S rRNA gene diversity at the end of the incubation period. (a) Cluster dendrogram of all gene sequences recovered with a universal 16S rRNA primer. Approximately unbiased probability (AU, red) and bootstrap probability (BP, green) are shown as percentages at nodes. (b) Relative abundances of the most abundant microbial groups classified at the level of family. ASVs with less than ten counts were grouped into the "Other" entegory. \*Archaea and bacteria that could only be classified at higher taxonomic levels are noted with an asterisk.

B1). In all three cases, clusters are supported by bootstrap values of 100, indicating organic carbon source was the major control on both archaeal and bacterial community composition. Archaea were the dominant populations observed in all

329 microcosms incubations, Bathvarchaeia made up the largest fraction of sequences in MMA microcosms incubations, which 330 was distinct from EtOH microcosms incubations that were dominated by Methanosarcinaceae (Fig. 5b). 331 MMA-amended microcosms incubations had Shannon Diversity Index values that were consistently higher than EtOH-332 amended mierocosms incubations (Fig. B2), indicating MMA amendment resulted in a more diverse microbial community. 333 Indicator Species Analysis performed at the taxonomic level of genus pointed to 68 bacterial and archaeal groups significantly 334 associated (p < 0.01) with MMA at high statistic values (> 0.95%). The EtOH treatments had only one indicator archaeal genus 335 with a similarly high statistic (0.983) and p-value (0.008): Methanosarcina (Table B1). Iron was not found to be a strong driver 336 of community structure with no indicator species identified for any iron treatment. In MMA microcosms incubations, three 337 genera comprised > 50% of the sequences regardless of iron treatment: Bathyarchaeia, Ca. Omnitrophaceae, and Marine 338 Benthic Group D/Deep Hydrothermal Vent Euryarchaeotal Group 1 (MBG-D/DHVEG-1). In EtOH microcosms incubations, 339 on the other hand, the top three genera, Methanosarcina, Syntrophotalea, and Bathyarchaeia, represented almost 75% of 340 recovered 16S rRNA sequences, in agreement with the lower diversity estimates in these treatments. We also looked for trends 341 within archaea and bacteria genera individually (Fig. 6). Two different genera of the family Methanosarcinaceae were found 342 to be indicators for carbon treatment (Fig. 6a). Methanosarcina was found to be an indicator for EtOH (statistic = 0.983; p-343 value = 0.008), while Methanococcoides was an indicator for MMA (statistic = 0.977; p-value = 0.004). Methanosarcina alone 344 represented > 50% of archaeal sequences in EtOH + hematite and EtOH + no iron treatments and they were the largest fraction 345 in the other iron treatments with EtOH amendment as well (Fig. 6a). The only other archaeal genera with significant 346 representation in EtOH microcosms incubations were Bathyarchaeia and Methanococcus (Fig. 6a). However, Bathyarchaeia 347 were found to be an indicator for MMA (statistic = 0.952; p-value = 0.005), not EtOH. They represented up to 51% of archaeal 348 sequences in MMA microcosms incubations. MBG-D/DVHEG-1 were also a larger fraction of the archaeal population in MMA 349 treatments. A group of unclassified archaea was consistently recovered from microcosms incubations with MMA treatments 350 as well (Fig. 5b, 6b). A BLAST search indicated these unclassified Archaea were most related to Ca. Thorarchaeota in the 351 Asgard superphylum (94–96% sequence similarity). None of these archaeal groups that represented the majority of archaeal 352 sequences in MMA bottles are of the "classical" orders of methanogens (Evans et al., 2019). This was unexpected as MMA 353 microcosms incubations produced significantly more measured methane than EtOH microcosms incubations. Classical 354 methanogens were found at very low relative abundance, e.g., Methanococcoides (avg. 1.9%) and Methanofastidiosales (avg. 355 0.7%). 356

Bacterial assemblages were more distinct between carbon treatments than archaeal assemblages (Fig. 6b). MMA treatments resulted in high relative abundances (up to 30%) of *Ca.* Omnitrophus followed by WOR-1 (also referred to as *Saganbacteria*; (Matheus Carnevali et al., 2019), *Lentimicrobiaceae*, MSBL5 (Mediterranean Sea Brine Lake Group 5), and *Sulfurovum* (Fig. 6b). While 6b). *Lentimicrobiaceae* are thought to be fermenters (Sun et al., 2016) and *Sulfurovum* sulfur reducing bacteria (Li et al., 2023; Wang et al., 2023), the metabolic capabilities and biogeochemical roles of *Ca.* Omnitrophus, *Saganbacteria*, and MBSL5 are largely unknown. The indicator with the highest statistic for MMA treatment, a member of the *Bacteroidetes*, was not highly abundant (Table B1). But *Ca.* Omnitrophus was also a strong indicator of MMA treatment (statistic = 0.976, p-

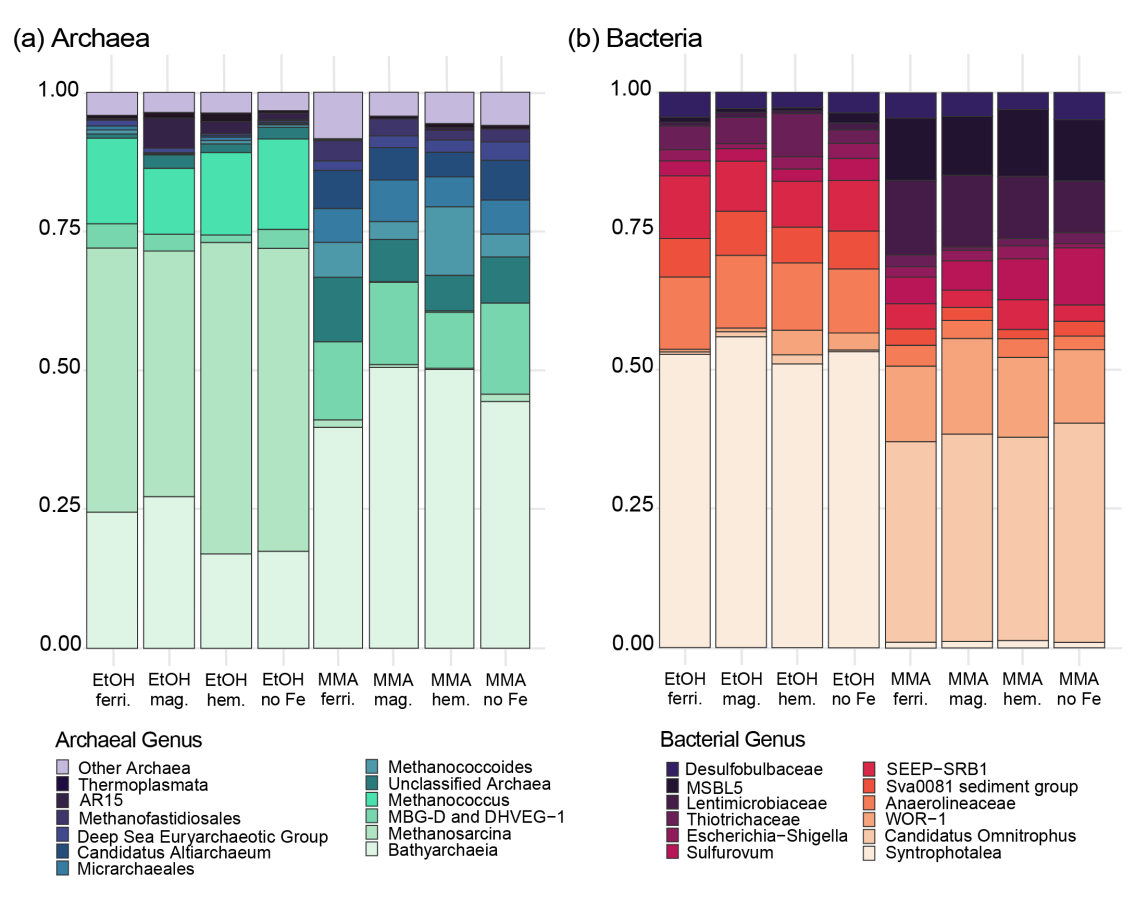
357

358

359

360

361



value = 0.009). In contrast, bacteria in EtOH incubations were dominated by *Syntrophotalea*, which made up ≥ 50% of bacterial sequences across all iron treatments (Fig. 6b). *Anaerolineaceae* was also a substantial proportion of the community in EtOH bottles. Both of these bacterial genera are likely involved in organic earbon fermentation (Hackmann, 2024; MeIlroy et al., 2017). Significant populations of Sva0081 sediment group and SEEP-SRB-1 were also found (Fig. 6b), both of which are sulfur reducers in the family *Desulfosarcinaceae* (Dyksma et al., 2018; Skennerton et al., 2017). Only *Syntrophotalea*, however, was found to be a strong indicator genus for EtOH treatment (statistic = 0.945, p-value = 0.009). No well known dissimilatory iron reducers or magnetotactic bacteria were found in our sequence data (Fig. 6b).

Figure 6. Most abundant bacterial (a) and archaeal (b) genera from each incubation group from the universal 16S primer dataset.

Bacterial data includes ASVs with 10 or more counts, and archaeal data includes ASVs that had 2 or more counts. 4 Discussion

# 4.1 Carbon source exerts a primary control on methane production

# 4.1.1 More methane production from non-competitive methylamine than ethanol

Our experimental design included two carbon treatments to investigate the effect of substrate competition on methane production from salt marsh microbial communities. We found that addition of a non-competitive, methylated organic carbon

reflects an adaptation of the natural microbial assemblage to the ready availability of methylated substrates in salt marshes. Methylamines are degradation products of common osmolytes synthesized by marsh grasses and other marsh organisms such as glycine betaine, proline betaine, choline and dimethylsulfoniopropionate (DMSP) (Cavalieri and Huang, 1981; Glob and Sørensen, 1987; King, 1988; Mulholland and Otte, 2002; Sørensen and Glob, 1987; Wang and Lee, 1994a). As such, methylamines are abundantly available in the sediment of salt marshes (Fitzsimons et al., 1997; Gibb et al., 1999; Lee and Olson, 1984; Oremland et al., 1982; Wang and Lee, 1994a; Yang et al., 1994). S. alterniflora has been shown to release methylamine to sediments (Wang and Lee, 1994), and 1994a) and, consistent with our results, active methylotrophic methanogens have previously been found in N. American salt marshes where S. alterniflora is native (Buckley et al., 2008; Cai et al., 2022; Franklin et al., 1988; Krause and Treude, 2021; Oremland et al., 1982; Oremland and Polcin, 1982; Parkes et al., 2012), consistent with our results. 2012a). Our results are also consistent with the shift from hydrogenotrophic to methylotrophic methanogenesis that was observed with the invasion of S. alterniflora into China's coastal salt marshes where it is not native (Yuan et al., 2016, 2019). GivenAlthough our 16S rRNA sequence data reflects the highermicrobial community at the end of the incubations rather than at the time point of highest methane production infor MMA microcosms incubations (Fig. 2a,c), itthese bottles continued to produce methane throughout the incubation period. It was therefore somewhat surprising to find that methylotrophic methanogens were not among the more abundant genera recovered in 16S rRNA sequences after incubation in bottles incubated with MMA amendments (Fig. 5b). In fact, all representatives of the classical orders of euryarchaeotal methanogens averaged only 0.6% of recovered sequences in MMA microcosms incubations across the four iron treatments. Instead, Bathyarchaeia was the most represented among the archaea by far (averaged 13% of all sequence reads in MMA microcosms incubations). As a class, Bathyarchaeia are found abundantly in anoxic marine sediments and terrestrial soils (Fillol et al., 20156; Zhou et al., 2018) where they are thought to be important methylotrophic acetogens that degrade a variety of organic carbon substrates (Farag et al., 2020; Hou et al., 2023). Methylotrophic It has been proposed that methylotrophic methanogenesis hasmay also been proposed be possible among the Bathyarchaeia based on genomic data (Borrel et al., 2016; Evans et al., 2015). However, but it has not yet been shown experimentally, and a recent study of existing metagenomes indicated that methanogenesis iswould not be widespread among them (Hou et al., 2023). Therefore, thereit is a possibility not likely that Bathyarchaeia contributes to produce methane production in MMA-amended incubations although this explanation it is not likely possible. A more likely source of the methane production in MMA incubations is a small but highly active population of classical methylotrophic methanogens. Such a that is highly active, despite representing a small proportion of the sequences recovered at the end of incubations. A small population of methanogens with high activity has been described previously in salt marsh sediments (Cai et al., 2022). Of the sequences we recovered from established methanogens, members of the genus Methanococcoides were most abundant (Fig. 6a). Methanococcoides have been identified in other studies of salt marsh sediments (Jameson et al., 2019; Jones et al., 2019; Munson et al., 1997) and they are known to utilize methylamines and other methylated compounds such as choline and glycine betaine, but not H<sub>2</sub> or acetate (L'Haridon et al., 2014; Liang et al., 2022;

substrate (MMA) yields more measurable methan a substrate that is fermented to acetate (EtOH) (Fig. 2a,c). This likely

376

377

378379

380

381

382

383

384

385

386

387

388

389

390

391

392

393

394

395

396

397

398

399

400 401

402

403

404

405

406407

classical methanogens, specifically Methanococcoides as the most abundant classical methanogen was, have also found been reported in seagrass meadow sediments where methylated compounds similarly fuel methane production via methylotrophic methanogenesis (Hall et al., 2024; Schorn et al., 2022). After Methanococcoides, Methanofastidiosales were the next most abundant of the established methanogens in MMAamended mierocosms incubations (Fig. 6a). Methanofastidiosales are restricted to methanogenesis through methylated thiol reduction (Nobu et al., 2016). Methanethiol, which can be formed as a degradation product of DMSP and methionine or by methylation of sulfide (Lomans et al., 2002), is also commonly available in salt marsh sediments (Carrión et al., 2019; Deévai and DeLlaune, 1995; Kiene and Visscher, 1987) and was likely to have been naturally present in the sediments used for our incubations. Notably, Methanofastidiosales were found along with Methanococcoides and Bathyarchaeia in methanecontainingmethanic sediments from seagrass meadows (Schorn et al., 2022). While the proportion of methanogen 16S rRNA sequences was lower overall in MMA treatments compared to EtOH treatments at the end of the incubations (Figs. 5b, 6a), the higher methane production rates observed with MMA likely indicates that a small population of salt marsh methanogens had high potential activity and was. They could have been primed to use non-competitive methylated substrates, such as methylamines and methanethiol, that are not accessible to sulfate- or iron-reducing bacteria. Methanogens in our incubations could also have been supported by the products of organic matter degradation by Bathyarchaeia, as has been reported previously in other iron-rich, sulfate-poor sediments (Ruiz-Blas et al., 2024).

Singh et al., 2005; Watkins et al., 2014). A similarly high relative abundance of Bathyarchaeia withand smaller abundance of

# 4.1.2 Ethanol yields a larger share of methanogens and potential eryptieconcurrent methane eyelingoxidation

MicrocosmsIncubations amended with EtOH also produced methane throughout the incubations, although less and later than with MMA amendments (Figs. 2, 3). EtOH would not directly support methanogens, but it can be fermented to methanogenic substrates by other members of the microbial community (Du et al., 2021; Schink, 1997). The lag in methane production in EtOH microcosmsincubations relative to MMA microcosmsincubations was likely related to this requirement that ethanol is converted to acetate or H<sub>2</sub> by bacteria before it could be utilized. The two most abundant bacteria in microcosmsincubations amended with EtOH<sub>T</sub> were Syntrophotaleaceae and Anaerolineaceae (Figs. 5b, 6b). Both of these bacterial genera are likely involved in organic carbon fermentation (Hackmann, 2024; McIlroy et al., 2017).), belong to fermentative families. Syntrophotalea was the most abundant bacterial genus by far (Fig. 6b) and was second most abundant among all taxa recovered from EtOH microcosmsincubations (12%–17%). Isolates of the genus Syntrophotalea (formerly Pelobacter) have been shown to ferment ethanol in the presence of a H<sub>2</sub>-scavenging methanogen and to produce acetate among their fermentation products (Eichler and Schink, 1985; Schink, 1984, 2006). More recently, a member of the Syntrophotalea was shown to transfer formate to a Methanococcus isolate in a mutualistic, methane-producing relationship (Day et al., 2022). Anaerolineaceae, although not as abundant, also likely contributed to fermentation in EtOH microcosmsincubations. They have been identified as primary fermenters capable of degrading carbohydrates, proteinaceous material or alkanes in anaerobic digesters (Bovio-Winkler et

al., 2020; Liang et al., 2015; McIlroy et al., 2017). In a few instances, they have also been found associated with acetoclastic methanogens from the *Methanothrix* (formerly *Methanosaeta*) genus (Liang et al., 2015; McIlroy et al., 2017).

Even though measured methane production was lower overall (Fig. 2c), and acetate and H<sub>2</sub> are competitive substrates available tothat can be consumed by both methanogen and non-methanogen members of the microbial community, classical methanogens represented a much larger share of the 16S rRNA sequences recovered at the end of EtOH microcosmsincubations (Fig. 5b). Methanosarcina was the dominant microbial genus, representing 15% to 25% of sequences recovered from EtOH incubations. Although Methanosarcina are capable of hydrogenotrophic, acetoclastic and methylotrophic methanogenesis, their ability to use acetate at high concentrations (Stams et al., 2019) was likely related to their successproliferation in EtOH-amended microcosmsincubations. Methanococcus, a genus of hydrogenotrophic methanogen, represented an additional 4 to 8% of total methanogen sequences in our EtOH microcosmsincubations (Fig. 6a). Their abundance allows for the possibility that a mutualistic relationship such as the one reported for Syntrophotalea and Methanococcus in an earlier study (Day et al., 2022), may have supported Methanococcus in our incubations as well. Although we did not find acetoclastic Methanothrix among the methanogens in our EtOH microcosmsincubations, it is possible that a similar cooperative interaction that was described between Anaerolineaceae and Methanothrix (Liang et al., 2015; McIlroy et al., 2017) formed between Anaerolineaceae and an acetoclastic Methanosarcina in our incubations.

While one explanation for the The larger proportion of methanogens observed in EtOH microcosms despite but lower methane production isobserved in EtOH incubations relative to MMA incubations could result from a less active population than the methylotrophic of methanogens than in MMA microcosms, it is also possible the MMA-amended bottles. However, an alternative explanation is that our measurements of methane concentrations underestimated methane production due to expetie methane evelingoxidation in EtOH microcosms incubations. Concurrent methane production and oxidation has been reported in salt marsh sediments (Krause et al., 2023, 2025; Krause and Treude, 2021; Segarra et al., 2013) as well in other coastal settings (Krause et al., 2023; Xiao et al., 2017, 2018). Methane oxidation is suggested by our identification of small numbers of ANME-3, which. Although ANME-3 were a small minority of sequences (included in "Other" in Fig. 6a), they were most represented in EtOH incubations with ferrihydrite, magnetite and hematite (0.41%, 0.3% and 0.48%, respectively). The We also detected the presence of the sulfate-reducing partner of anaerobic methanotrophs, SEEP-SRB1 (Schreiber et al., 2010; Skennerton et al., 2017), in all EtOH-amended microcosms also suggests anaerobic methane oxidation occurred (Fig. incubations (Fig. 6b). Although sulfate-free artificial seawater was used to make up our sediment slurry, natural reduced sulfur of multiple forms was identified in the marsh creek sediments (Fig. 1b), and 1b). Although we did not measure sulfur species during the incubations and reduced sulfur native to the sediments would have been diluted by our use of sulfate-free artificial seawater, sulfur cycling is suggested by the presence of sulfur oxidizing *Thiotrichaceae* (Ravin et al., 2023) in addition to the sulfate-reducing Desulfosarcinaceae (Fig. 5b). It is also possible that sulfate-reducing bacteria were reducing Fe(III) in our incubations (Coleman et al., 1993; Lovley et al., 1993), or anaerobic methane oxidation could be coupled to Fe(III) reduction (Cai et al., 2018; Ettwig et al., 2016; Yu et al., 2022) as this), which has been observed previously in salt marsh sediments (Krause and Treude, 2021; Segarra et al., 2013). Overall, a picture emerges of a complex web of interspecies interactions mediated by multiple indirect electron shuttles and redox-active species in EtOH microcosms incubations.

# 4.2 Conductive minerals promote increased methylotrophic methane production

We expected EtOH microcosmsincubations to reveal the potential for IET to enhance methane production by salt marsh microbial communities based on the results of previous studies—that described IET. Many studies of co-cultures and enrichments in which IET was found use ethanol to enrich the bacterial and methanogen partners and to support methane production (Kato et al., 2012; Rotaru et al., 2014a2019, 2014, 2018, 2019; Tang et al., 2016). Transfer of electrons between methanogens and electroactive bacteria has been shown through both magnetite and hematite (Aromokeye et al., 2018; Kato et al., 2012; Zhou et al., 2014). But (semi)conductive iron minerals have also been shown to enhance the activity of acetoclastic methanogens themselves, without a bacterial partner (Fu et al., 2019; Wang et al., 2020; Xiao et al., 2021). The typical methanogen involved in either pathway that accelerates methane production is from the metabolically versatile genus Methanosarcina or the acetoclastic genus Methanothrix (Rotaru et al., 2021; Xiao et al., 2021). Although we did not detect Methanothrix, Methanosarcina was abundantly represented in our EtOH microcosmsincubations (Fig. 5b). However, we did not observe any definitive increase in methane production in the presence of either magnetite or hematite relative to no iron amendments in EtOH microcosmsincubations (Fig. 2d). This suggests IET was not active in EtOH microcosmsincubations. Genera of well-known electroactive bacteria (Garber et al., 2024; Lovley and Holmes, 2022) were also not detected in EtOH microcosmsincubations.

Instead, the most methane produced and highest methane production rates that we observed were found in MMA + magnetite microcosmsincubations followed by MMA + hematite microcosmsincubations in the first 10 days (Figs. 2,3). Although methane production with no iron amendment was variable, the average among replicates was lower than that with magnetite or hematite amendments and methane production with MMA + ferrihydrite was significantly lower. This pattern of higher methane production rates with magnetite and hematite than with ferrihydrite or no iron has been reported previously in rice paddy soil microbial enrichments (Kato et al., 2012; Zhou et al., 2014). However, the most abundant methanogens in MMA incubations with these iron treatments were neither *Methanosarcina* nor *Methanothrix*. A few other methanogenic genera have been found capable of participating in IET (e.g., *Methanobacterium*; (Zheng et al., 2020, 2021), suggesting the full diversity of IET-capable methanogens is not yet known. Methylotrophic methanogens, such as those that were most abundant in our MMA microcosmsincubations (Fig. 6a), have not been identified as capable of IET to date, however. Still, *Methanococcoides* are a member of *Methanosarcinales*, an order with other IET-capable genera. Some *Methanococcoides* species have been found with cytochromes (Jussofie and Gottschalk, 1986; Saunders et al., 2005) that could facilitate extracellular electron transfer.

The bacterial partner in IET interactions is more variable and therefore more difficult to predict. In studies of IET-active cocultures and enrichments, *Geobacter* is often the syntrophic partner of methanogens and can be found in high abundance, but not always (Deng et al., 2023; Holmes et al., 2017; Kato et al., 2012; Liu et al., 2015; Rotaru et al., 2014b; Zhou et al., 2014). We did not recover 16S rRNA sequences belonging to Geobacter or other bacterial genera that are found in syntrophic association with methanogens (e.g., Syntrophomonas : Yuan et al., 2020; Zhao et al., 2018) or Rhodoferax : Yee and Rotaru, 2020; Zhao et al., 2020). Instead, the most abundant bacterial genus was Ca. Omnitrophus (Fig. 6b). Ca. Omnitrophus has widespread distribution in the environment, but they have remained relatively uncharacterized. Members of the Ca. Omnitrophus genus have been associated with metal-contaminated groundwater (Bärenstrauch et al., 2022) and magnetite production (in the form of magnetosomes. (Kolinko et al., 2016; Lin et al., 2018). In the class Omnitrophia, metagenomic evidence indicates potential to produce cytochromes for use in dissimilatory metal reduction and conductive pili (Perez-Molphe-Montoya et al., 2022; Seymour et al., 2023). These features allow for the possibility that Ca. Omnitrophus are the electroactive syntrophic partner of Methanococcoides in our MMA incubations. However, Ca. Omnitrophus was also found abundantly in MMA incubations with no iron and ferrihydrite treatments (Fig. 6b), and these incubations did not appear to have active IET. The other bacterial genera with the highest abundances, WOR-1, or Saganbacteria, Lentimicrobiaceae, MSBL5, and Sulfurovum (Fig. 6b) are less likely to be the electroactive bacterial partner. Lentimicrobiaceae are thought to be fermenters (Sun et al., 2016), Sulfurovum are sulfur reducing bacteria (Li et al., 2023; Wang et al., 2023), and metabolic capabilities and biogeochemical roles of Saganbacteria, and MBSL5 are largely unknown. Like Ca. Omnitrophus, the abundances of these genera are also not distinctly different between bottles with magnetite and hematite amendments vs. bottles with ferrihydrite and no iron amendments. Despite the distinctly higher methane production rates early on, the microbial communities in MMA + magnetite and MMA + hematite microcosms incubations were not significantly different from MMA + no iron and MMA + ferrihydrite by the end of the incubations. The similar bacterial assemblages in MMA microcosms incubations may reflect similar methane production rates at the end of the incubations (Fig. 3) or they could be explained by the microbial community responding to the small amount of magnetite naturally present in salt marsh sediments (Fig. 4).

#### 4.3 Magnetite formation from ferrihydrite with ethanol supplementation

508

509

510

511

512

513

514

515

516

517

518

519

520

521

522

523

524

525

526

527528

529

530

531

532

533

534

535

536

537

538

539

540

Despite general similarities in methane production and microbial community composition in all microcosms incubations with the same organic carbon amendment, large quantities of magnetic minerals were produced in only one of our incubations: EtOH + ferrihydrite (Figs. 4, C1). Coercivity, remanent coercivity, and coercivity spectra suggest the mineral is magnetite, and that the magnetite produced in EtOH + ferrihydrite incubations was different from that natively present in marsh creek sediments (Fig. 4c,d). The low coercivity suggests very fine-grained magnetite (above 25 nm but probably not over 80 nm; (Dunlop, 1973; Dunlop and Ozdemir, 2001]; Enkin and Dunlop, 1987). It is also lower coercivity than seen in magnetosomes suggesting extracellular precipitation (Bai et al., 2022; Egli, 2004; Xue et al., 2024). Such a transformation of ferrihydrite is not surprising considering that iron-reducing bacteria are known to facilitate the conversion of poorly crystalline Fe(III) minerals to more crystalline iron-bearing minerals such as magnetite (Benner et al., 2002; Hansel et al., 2003; Zachara et al., 2002). However, no detectable magnetite was formed beyond natural abundance in the sediment from ferrihydrite during incubation with MMA + ferrihydrite (Fig. 4a) even though Fe<sup>2+</sup> concentrations were elevated during the incubation indicating

that iron reduction occurred (Fig. 2b)), and there was a slightsmall delay in methane production, indicating that iron reduction was competing with methanogenesis early in the incubations (Fig. 2a). Although the mineral fate of Fe(II) produced by iron reducers has been tied to the rate of iron reduction (Kappler et al., 2023), microcosmsincubations with EtOH + ferrihydrite, MMA + ferrihydrite and EtOH + magnetite treatments all produced similar amounts of net Fe<sup>2+</sup> (Fig. 2b,d) suggesting similar iron reduction rates. Microbial community composition did not provide strong clues as to the identity of the bacteria responsible for magnetite formation either. There was no significant difference between the bacterial community in the EtOH + ferrihydrite incubation and other EtOH treatments (Fig. 6b). No well-known dissimilatory iron reducers (or magnetotactic bacteria) were among the bacterial genera that we recovered from EtOH incubations (Bazylinski et al., 2013; Kappler et al., 2021; Simmons and Edwards, 2007b; Zhao et al., 2024):2007a; Zhao et al., 2025), with the exception of Ca. Omnitrophus. In contrast to MMA incubations, however, only a small fraction of sequences in EtOH incubations were from Ca. Omnitrophus. Although the genus Ca. Omnitrophus does include magnetotactic bacteria (Kolinko et al., 2016; Perez-Molphe-Montoya et al., 2022), they were much less abundant in EtOH incubations than MMA incubations. There is a possibility that bacteria of the genus Methanosarcina, which were highly abundant in EtOH incubations, are directly involved in iron reduction and ferromagnetic mineral formation as cultures of Methanosarcina barkeri have been shown capable of ferrihydrite reduction (Bond and Lovley, 2002; Sivan et al., 2016; Yu et al., 2022).

In rice paddy soils, transformation of ferrihydrite to magnetite results in an eventual enhancement in methane production (Tang et al., 2016; Zhuang et al., 2015, 2019), but the impact of magnetite formation on methane production has not been characterized yet in salt marshes. We did not observe a similar increase in methane production following magnetite formation in EtOH + ferrihydrite microcosmsincubations as that observed in rice paddy incubations, at least on the timescale of our 4034-day incubations. However, this may result from a mismatch between the more prolific methylotrophic methane producers in our salt marsh incubations and the formation of magnetite, which only occurred in EtOH incubations. Although we did not detect magnetite formation in MMA + ferrihydrite microcosmsincubations, the widespread presence of crystalline iron minerals at anoxic and euxinic depths resulting from transformation of amorphous iron minerals has been reported previously (Kostka and Luther, 1995; Taillefert et al., 2007). Separate populations of iron reducing bacteria accessing different carbon substrates may be involved in magnetite formation and IET in salt marshes. The activity of both would influence rates and quantities of methane production by methylotrophic methanogens.

## 5 Conclusions

In this study, we hypothesized that the noncompetitive, methylated substrate MMA would yield more methane production than EtOH without the addition of iron oxide minerals, but that the acetoclastic methanogens that we expected to find in EtOH microcosmsincubations would respond to the presence of (semi)conductive iron oxides with increased methane production while methylotrophic methanogens in MMA microcosmsincubations would not. Instead, we found that a noncompetitive substrate and the presence of conductive minerals worked in concert to yield the highest methane production from salt marsh

microbial communities. Methanogens in salt marshes therefore can employ multiple simultaneous strategies to circumvent the redox ladder. Adding a methylated organic carbon substrate had a stronger effect on measured methane production and on the microbial community than the presence of conductive minerals. This suggests that it is not just the presence of sulfate in polyhaline salt marshes that controls methane production, but also the contribution of methyl-containing osmolytes from marsh plants and animals that support methane production in higher-salinity coastal environments. The transformation of ferrihydrite to magnetite and the persistent presence of crystalline iron minerals in anoxic zones of salt marsh sediments could further enhance methane production in salt marshes. The importance of these multiple factors and their inevitable variability across space, depth and seasons are likely to contribute to the heterogeneity that has been observed in methane emissions from salt marshes.

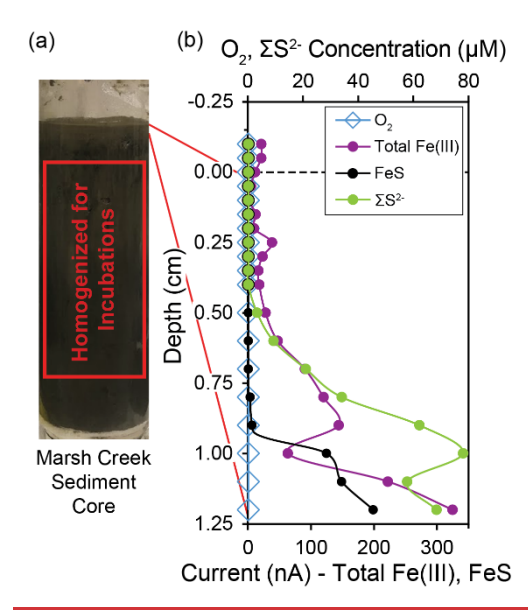


Figure 1: Redox conditions and sampling depths in the marsh creek sediment core. (a) Photo of 22.5 cm sediment core before extrusion with interval of sediment used for incubations highlighted. (b) Microelectrode profiles of oxygen, iron and sulfur species with depth in the sediment core as measured by cyclic voltammetry. Total Fe(III) is the summed peak areas for Fe(III)(aq), Fe(III)(s) nanoparticles of multiple sizes, and Fe(III) with organic ligands. Total Fe(III) and FeS are plotted with relative units. Traces of FeS were detected beginning at 0.5 cm. O<sub>2</sub>, Fe<sup>2+</sup>, and HS<sup>-</sup> were not detected in the sediment core or overlying water. The dashed line at 0 cm represents the sediment water interface and negative depths represent height in overlying water.

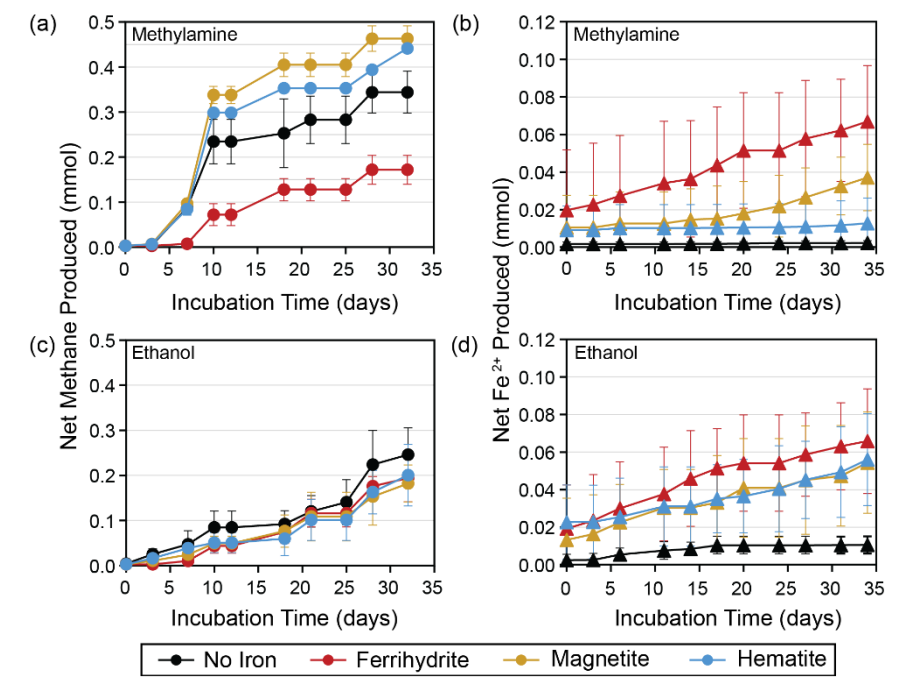


Figure 2: (a) Net methane and (b) Fe<sup>2+</sup> produced with methylamine amendments and all iron treatments averaged over three replicates. Similar plots for (c) net methane and (d) Fe<sup>2+</sup> produced with ethanol amendments are also averaged over three replicates. Error bars represent the standard deviation from the replicates' average value.

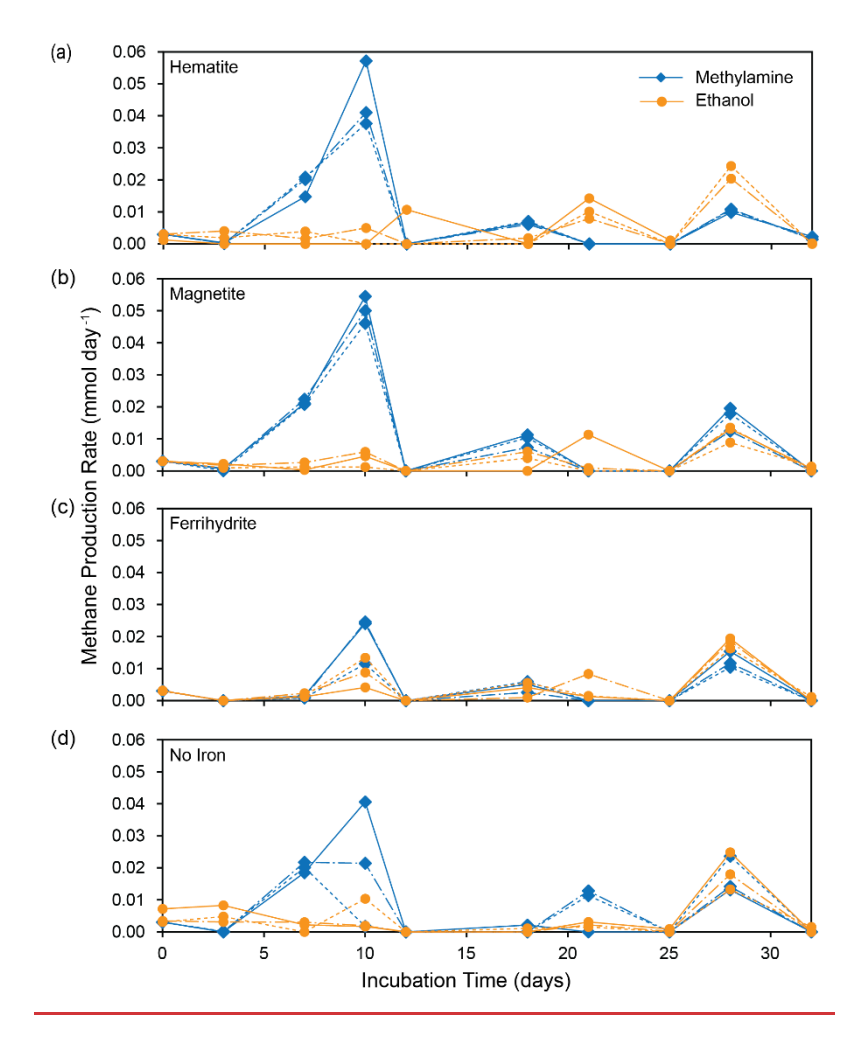


Figure 3: Methane production rates for each replicate incubation bottle shown for MMA incubations (blue) and EtOH incubations (orange) separated by iron treatment.

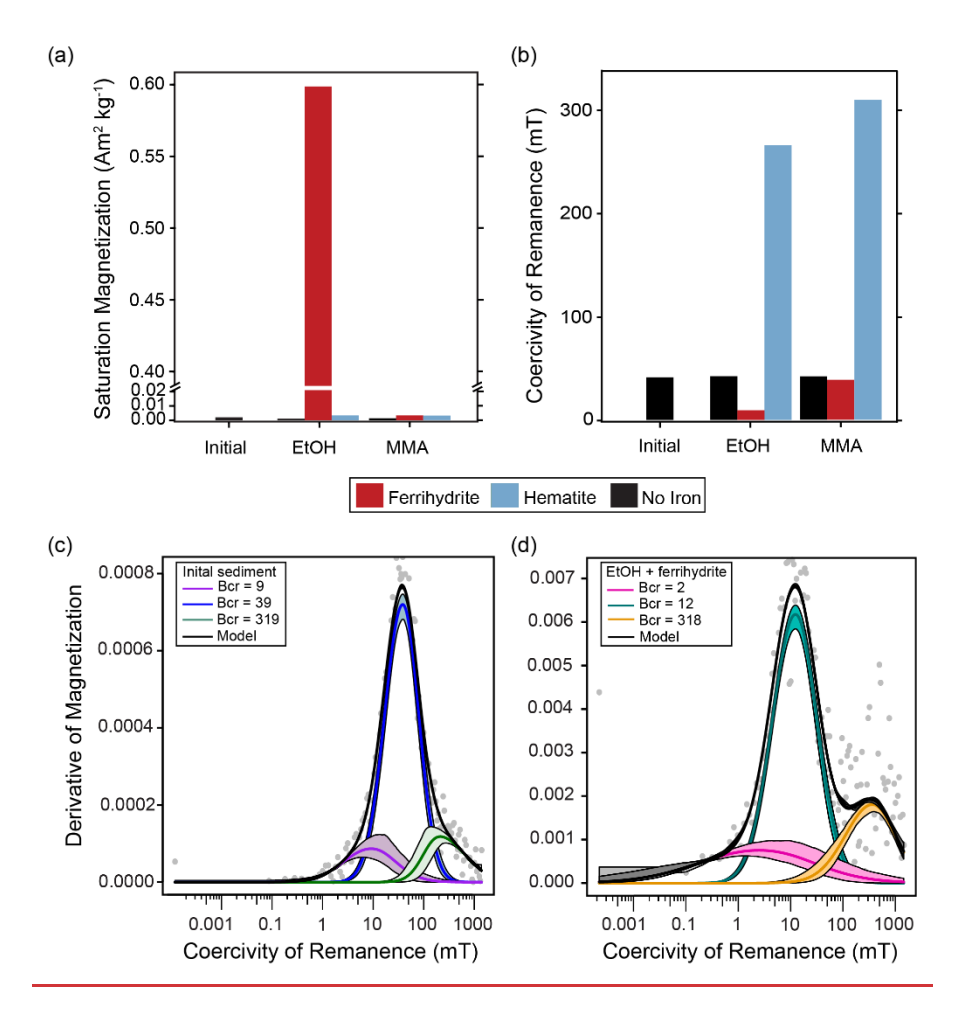


Figure 4: Ferromagnetic mineral measurements of initial homogenized sediment used in all incubations and sediment recovered from all amended incubations at the end of the incubation period. (a) Abundance of ferromagnetic minerals as indicated by saturation magnetization (Ms; Am² kg⁻¹ of dried sediment sample). (b) Mineral identification summarized by coercivity of remanence (Bcr; mT). Examples of MAX UnMix data for (c) initial sediment with no iron mineral amendment and (d) EtOH + ferrihydrite sediment at the end of the incubation period. Data from sediments amended with magnetite are not shown as magnetite amendment itself overwhelmed any signals of magnetite formation or loss.

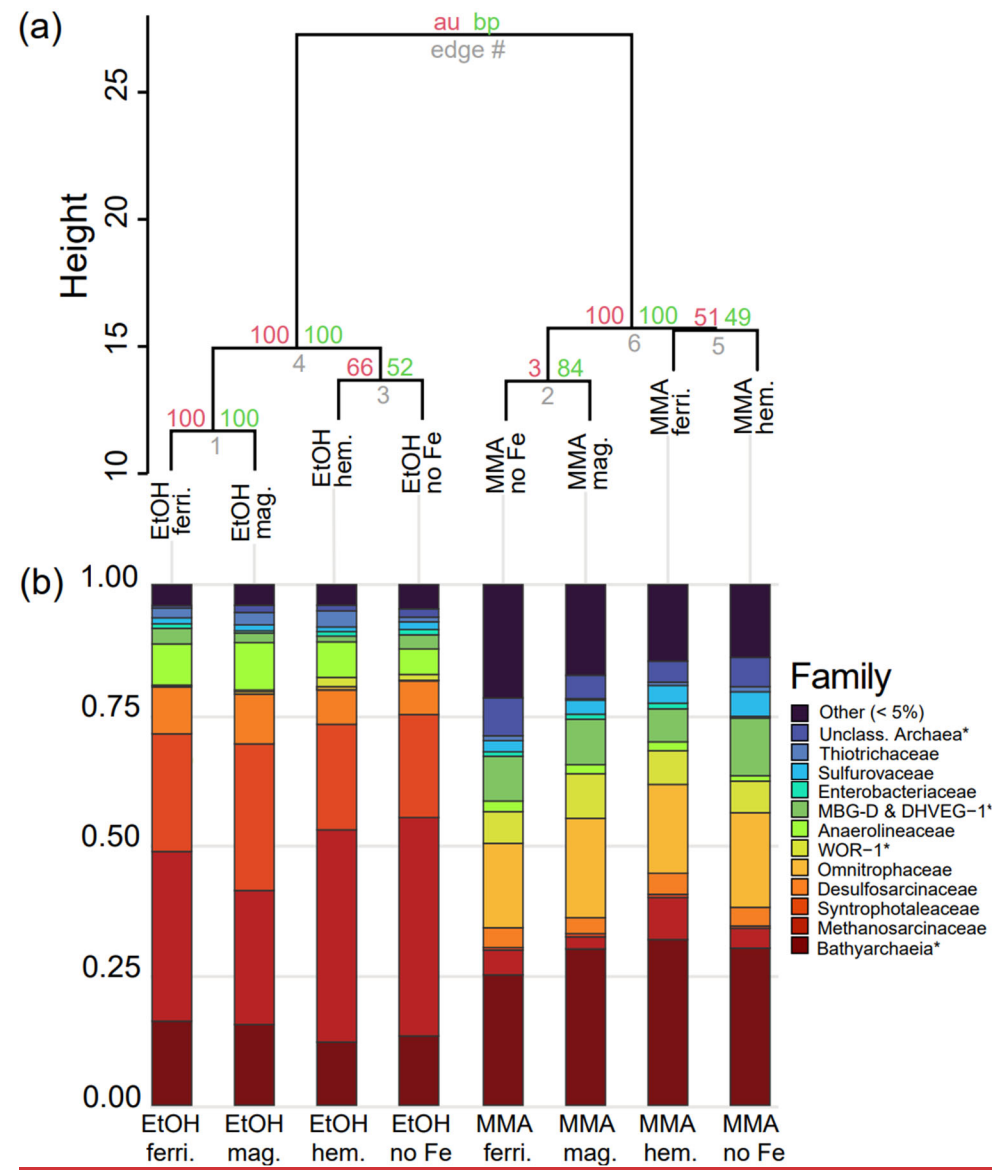


Figure 5: Microbial community composition from 16S rRNA gene diversity at the end of the incubation period. (a) Cluster dendrogram of all gene sequences recovered with a universal 16S rRNA primer. Approximately unbiased probability (AU, red) and bootstrap probability (BP, green) are shown as percentages at nodes. (b) Relative abundances of the most abundant microbial groups classified at the level of family. ASVs with less than ten counts were grouped into the "Other" category. \*Archaea and bacteria that could only be classified at higher taxonomic levels are noted with an asterisk.

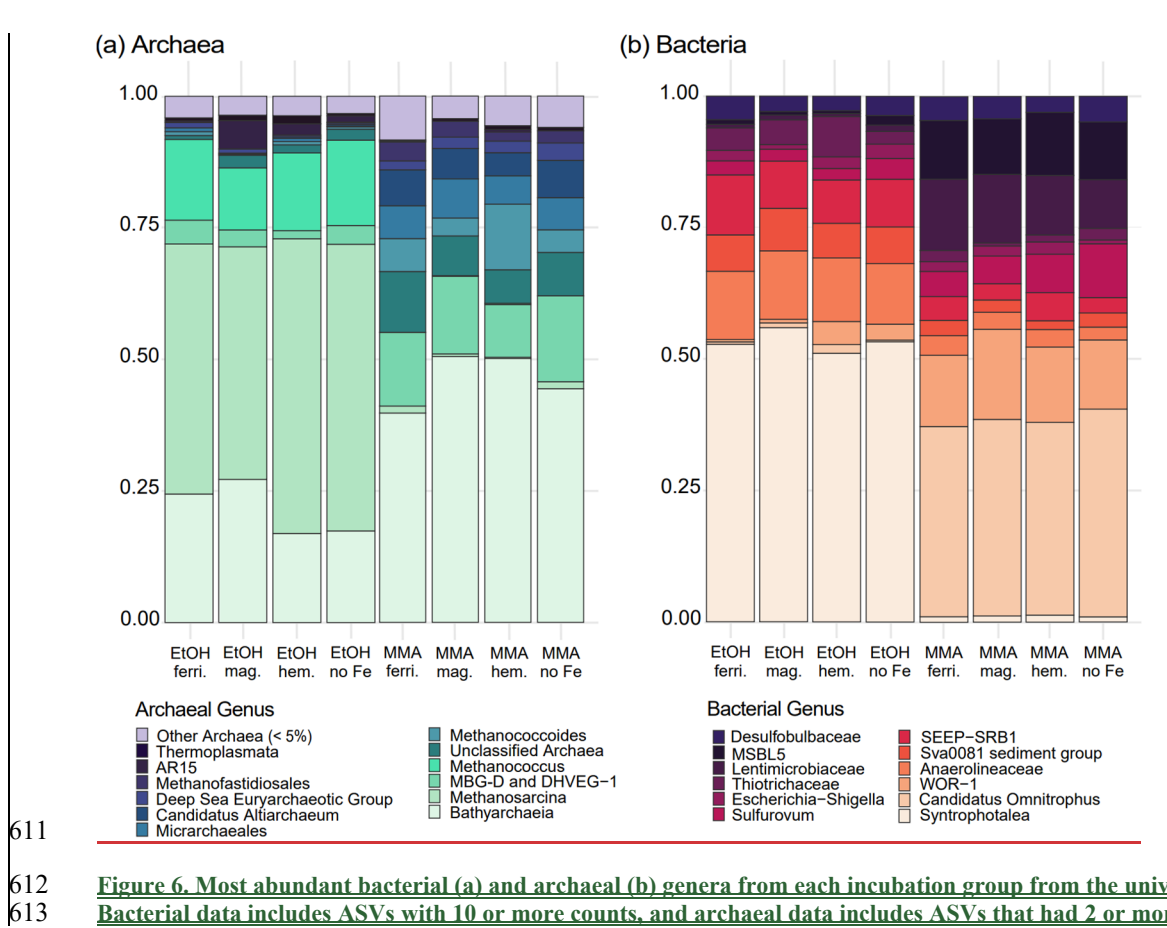
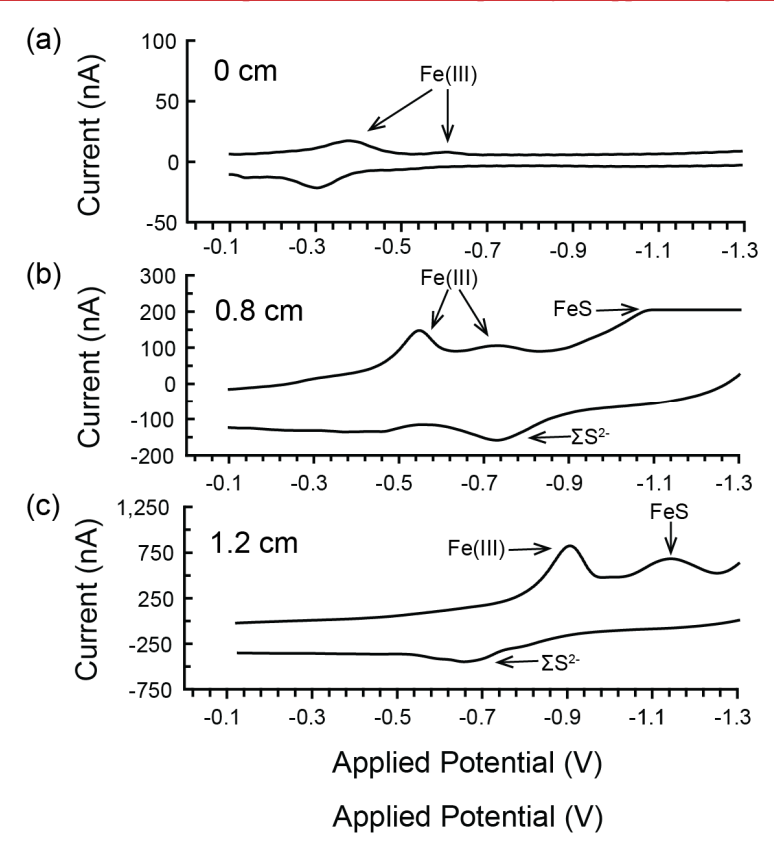


Figure 6. Most abundant bacterial (a) and archaeal (b) genera from each incubation group from the universal 16S primer dataset. Bacterial data includes ASVs with 10 or more counts, and archaeal data includes ASVs that had 2 or more counts.



**Appendix A: Extended Cyclic Voltammetry Results** 

Figure A1: Example voltammograms from depths of distinct redox conditions for (a) the sediment-water interface at 0 cm, (b) 0.8 cm depth and (c) 1.2 cm depth in the sediment. Traces of FeS are detected beginning at 0.8 cm, however, the small peak shown (b) is almost entirely off scale.

# Appendix B: Extended Results from DNA Analysis

Indicator classes for	r Genus		p-value	
Ethanol	Methanosarcina	0.983	0.0083	
	Methanococcus	0.945	0.0094	
	Syntrophotalea	0.937	0.0094	
	SCGC AAA286-E23	0.933	0.0330	
	Syntrophotalea	0.924	0.0063	
Methylamine	Bacteroidetes BD2-2	0.981	0.0089	
	Methanococcoides	0.977	0.0040	
	Candidatus Omnitrophus	0.976	0.0089	
	Rs-M47	0.974	0.0089	
	MSBL5	0.974	0.0060	
	Roseimarinus	0.974	0.0089	
	SBR1031	0.971	0.0065	
	661239	0.970	0.0065	
	DSEG	0.961	0.0038	
	Marinimicrobia (SAR406 clade)	0.961	0.0089	
	Desulfatiglans	0.961	0.0089	
	Unclassified Archaea	0.959	0.0089	
	Bathyarchaeia	0.952	0.0054	
	CK-2C2-2	0.951	0.0089	

Table B1. Indicator genera for carbon and iron treatments based on 16S rRNA classified at the level of genus. Because of the large number of indicators found for methylamine treatment, only genera with a statistic value of 0.95 or greater are included for this category.

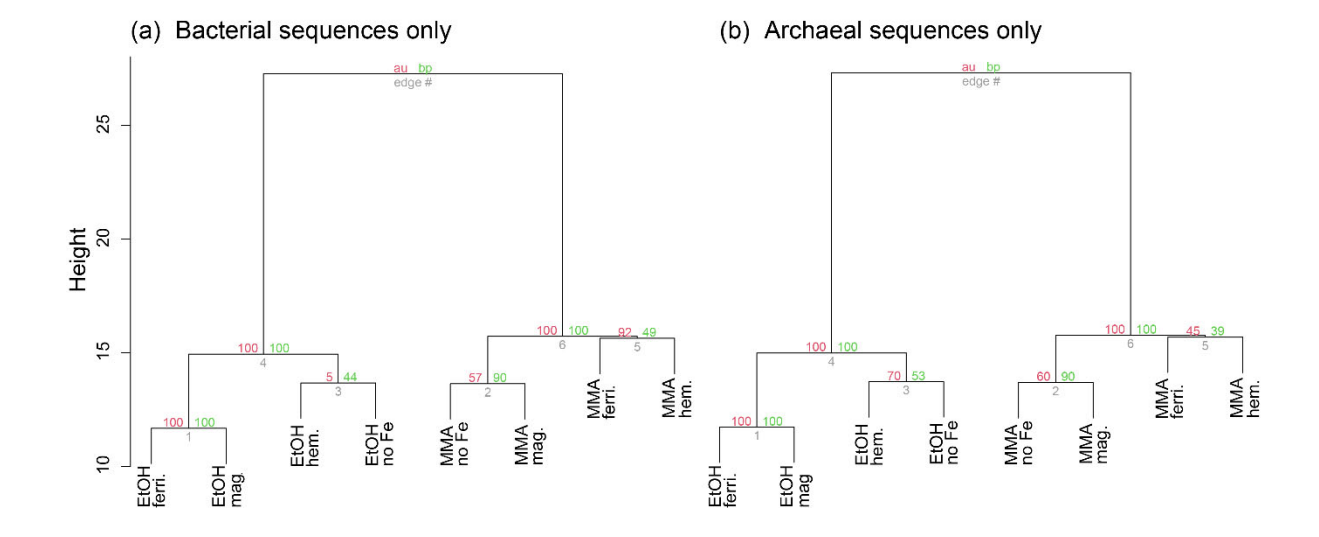
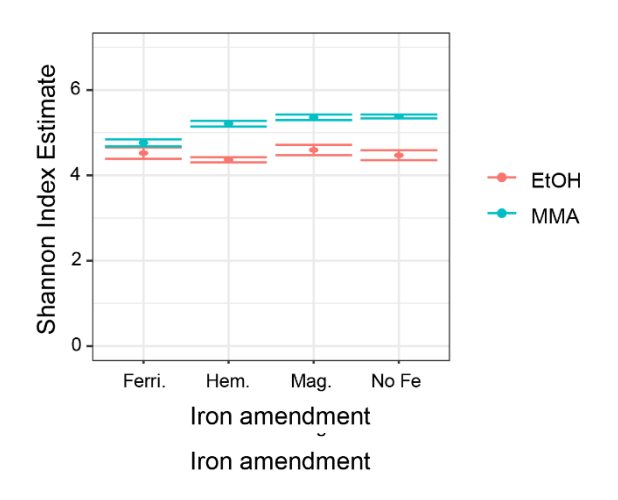


Figure B1: Cluster dendrograms for DNA-based 16S rRNA gene diversity sorted only to the (a) Domain Bacteria and the (b) Domain Archaea. Approximately unbiased (AU) p-values are in red (in percentage), and bootstrap probability (BP) values are shown in green.



638 Figure B2: Shannon Diversity Index values for microbial assemblages at the end of the incubation period.

# Appendix C: Extended Results and Discussion of Magnetics Analyses

**Sediments from Incubations amended with Hematite**. A higher saturation magnetization was observed in the MMA + hematite treatment compared to the EtOH + hematite treatment. Coercivity spectra are similar between the two treatments with two clear magnetic phases (hematite and magnetite), but the relative ratios of magnetite and hematite differ slightly. The ratio is 43:57 in the EtOH + hematite treatment versus 37:63 in the MMA + hematite treatment. This is reflected in the slightly lower coercivity values in the EtOH + hematite treatment than the MMA + hematite treatment (Fig. 4b, Table C1).

Sample Description	Saturation Magnetization (M <sub>s</sub> , Am <sup>2</sup> kg <sup>-1</sup> )	Saturation Remanent Magnetization (Mrs, Am <sup>2</sup> kg <sup>-1</sup> )	Coercivity (B <sub>c</sub> , mT)	Coercivity of Remanence (B <sub>cr</sub> , mT)
Ferrihydrite (synthesized)	0.340179	0.000145813	0.606429	95.2
Magnetite (standard)	88.4135	9.0119	11.8811	36.324
Hematite (standard)	0.369133	0.122205	381.008	650.458
Sediment + no amendments	0.001858	0.000415673	15.0399	41.1813
MMA + no iron	0.001299	0.000322783	15.9069	42.0022
MMA + ferrihydrite	0.003299	0.000564935	15.1455	38.6557
MMA + magnetite	3.61366	0.225262	6.91942	22.5718
MMA + hematite	0.00305543	0.00122488	50.5933	309.928
EtOH + no iron	0.001077	0.000356518	19.5832	42.3108
EtOH + ferrihydrite	0.598696	0.0057064	0.540556	9.24095
EtOH + magnetite	2.69794	0.182766	7.7745	30.1945
EtOH + hematite	0.003332	0.00128976	47.9657	265.949

Table C1. Magnetics measurement results for iron minerals and all incubations at the beginning of the incubation periods (sediment + no amendments) and at the end of the incubation period (all other incubations).

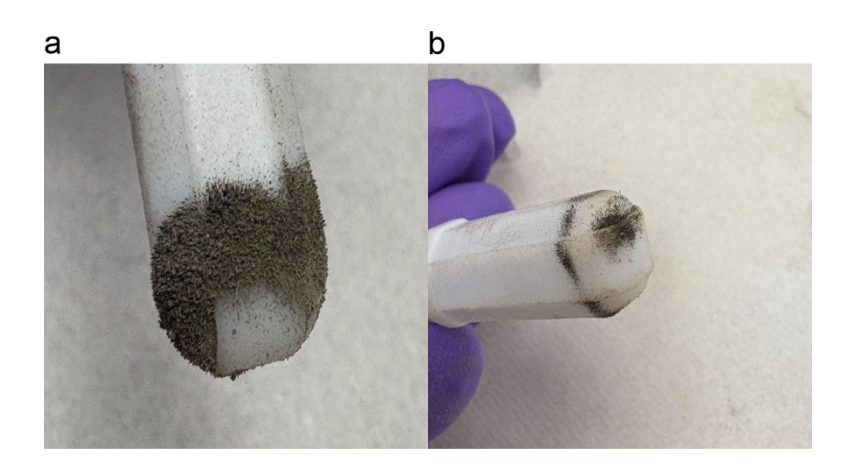
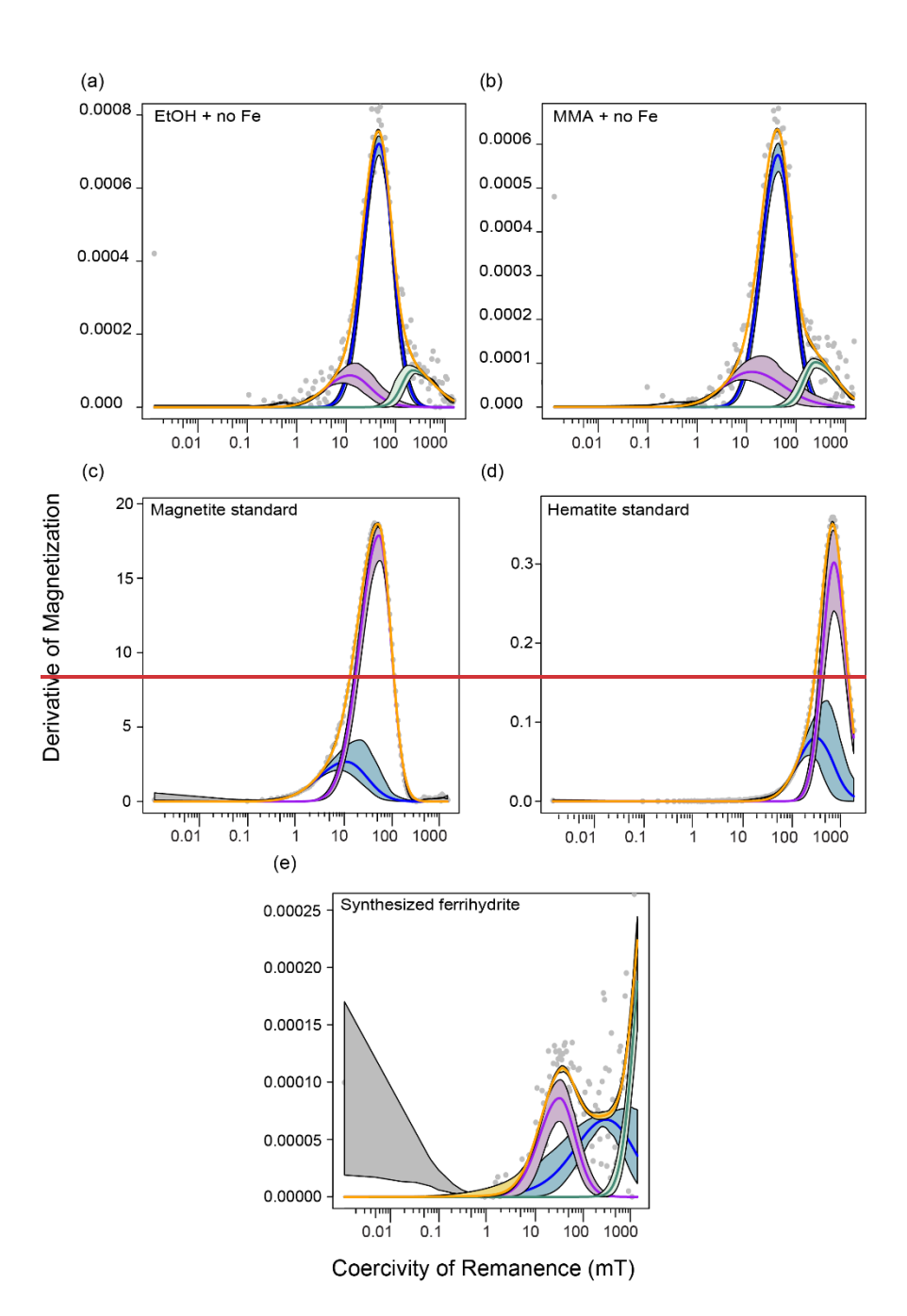


Figure C1: Photo of ferromagnetic minerals pulled out of freeze-dried sediment with a magnetic stirbar. These sediments were recovered from EtOH + ferrihydrite incubations at the end of the incubation period. The magnetic mineral sticking to the stirbar is likely magnetite and/or greigite. (a) Stirbar with magnetic mineral and sediments. (b) Stirbar after sediments had been tapped off, more selectively leaving the magnetic mineral attached.



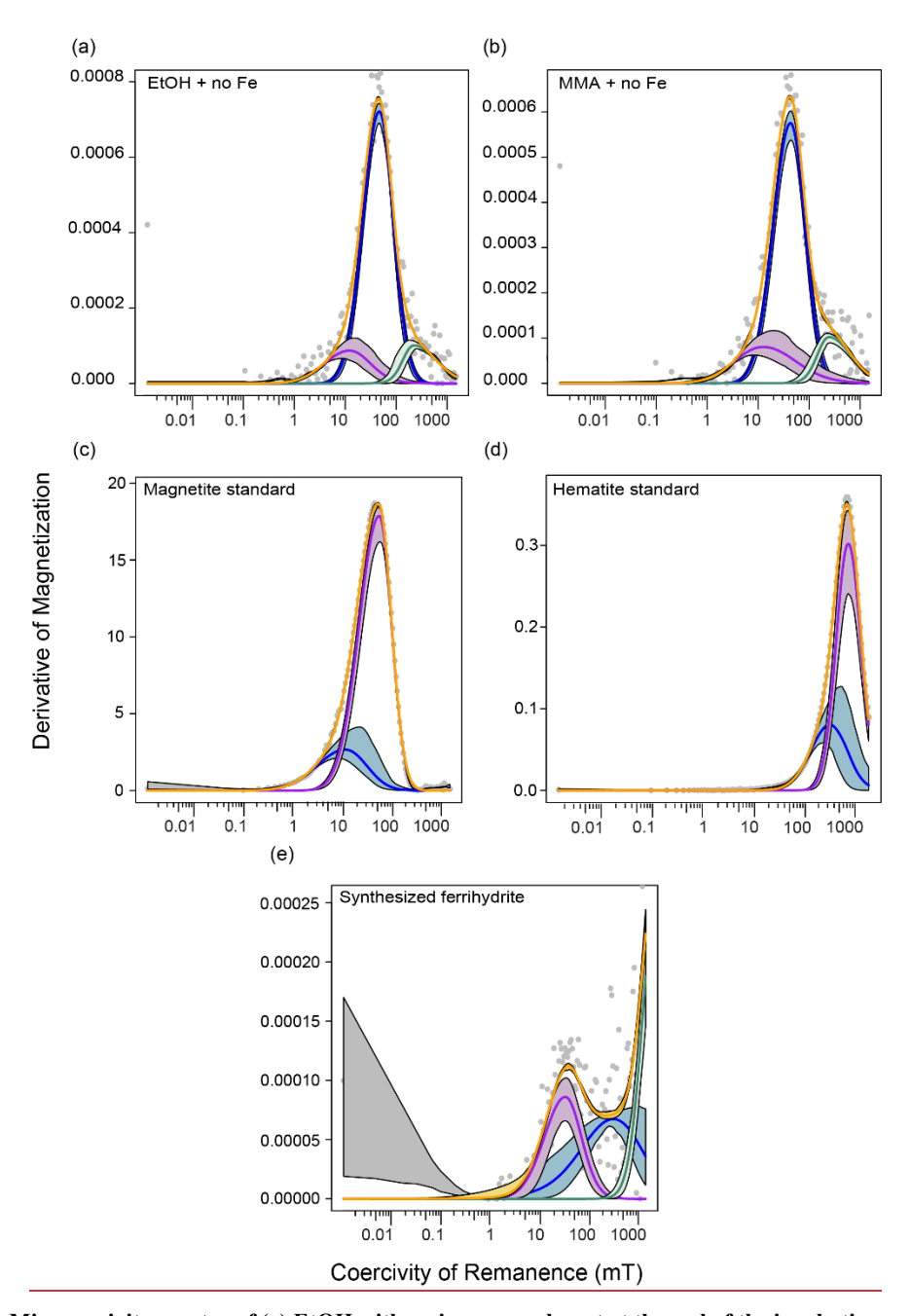


Figure C2: MAX UnMix coercivity spectra of (a) EtOH with no iron amendment at the end of the incubation period, (b) MMA with no iron amendment at the end of the incubation period, (c) the magnetite standard used in all magnetite-containing incubations, (d) the hematite standard used in all hematite-containing incubations and (e) the synthesized ferrihydrite used in all ferrihydrite-containing incubations. Because ferrihydrite is only weakly ferromagnetic, there is high noise in the data making it difficult to deconvolve a peak.

667	Code	Availal	bility
-----	------	---------	--------

- 668 Rmd file used to generate all DNA figures and data tables found can be at:
- 669 -https://hansonlabgit.dbi.udel.edu/hanson/block et al manuscript.git.

# 670 **Data Availability**

672

678

680

688

Amplicon sequence data is available at: -https://www.ncbi.nlm.nih.gov/bioproject/PRJNA1200716/.

## **Author Contribution**

- 673 This project was conceptualized by S.R.S.W. with the input of K.R.B. and A.A. Development of methodology and
- 674 investigation was done by K.R.B, A.A and S.R.S.W. All authors contributed to data curation and formal analyses. Data
- visualization was done by K.R.B., S.R.S.W., T.E.H. and S.P.S. Original draft preparation was done by K.B. and S.R.S.W. All
- authors contributed to reviewing and editing the manuscript. Funding acquisition, project administration and supervision were
- done by S.R.S.W.

## **Competing Interests**

The authors declare that they have no conflict of interest.

## Acknowledgements

- 681 Undergraduate interns participating in an NSF-supported Marine Sciences REU program over multiple years contributed to
- the development of this project: Sarah Bartoloni in 2019, Ethan Goulart in 2021 and Samantha Reynolds in 2024, as well as
- an undergraduate intern participating in the UD Summer Scholars program, Matthew Hicks, in 2021. Particular thanks is owed
- 684 to S. Reynolds for her contributions and discussions during the writing of this manuscript. We also thank lab members Justin
- 685 Guider, Sawyer Hilt and Leland Wood, for their assistance with field work, Andrew Wozniak for the use of his GC-FID
- 686 instrument and Jennifer Biddle for her advice and suggestions during the years of iterative improvement. Our manuscript was
- 687 significantly improved by helpful discussions about cyclic voltammetry data interpretation with Mustafa Yücel.

## Financial Support

- The development of this project was supported by NSF OCE-2342979 to S.R.S.W. The participation of A.A. and previous
- 690 undergraduate interns were made possible by the UD Marine Sciences Research Experiences for Undergraduates (REU)

- program administered by Joanna York (NSF OCE-2051069). K.B. was supported by NSF OCE-2342979 as well as University
   of Delaware Graduate Scholars Award.

## 695 References

- 696 Al-Haj, A. N. and Fulweiler, R. W.: A synthesis of methane emissions from shallow vegetated coastal
- 697 ecosystems, Glob. Chang. Biol., 26, 2988–3005, doi:10.1111/gcb.15046, 2020.
- Antler, G., Mills, J. V., Hutchings, A. M., Redeker, K. R., and Turchyn, A. V.: The Sedimentary Carbon-Sulfur-
- 699 Iron Interplay A Lesson From East Anglian Salt Marsh Sediments, Front Earth Sci., 7, 140,
- 700 doi:10.3389/feart.2019.00140, 2019.
- Apprill, A., McNally, S., Parsons, R., and Weber, L.: Minor revision to V4 region SSU rRNA 806R gene primer
- greatly increases detection of SAR11 bacterioplankton, Aquat. Microb. Ecol., 75, 129–137, doi:10.3354/ame01753,
- 703 2015.
- 704 Aromokeye, D. A., Richter-Heitmann, T., Oni, O. E., Kulkarni, A., Yin, X., Kasten, S., and Friedrich, M. W.:
- 705 Temperature Controls Crystalline Iron Oxide Utilization by Microbial Communities in Methanic Ferruginous
- Marine Sediment Incubations, Front. Microbiol., 9, 2574, doi:10.3389/fmicb.2018.02574, 2018.
- Bai, F., Chang, L., Pei, Z., Harrison, R. J., and Winklhofer, M.: Magnetic biosignatures of magnetosomal greigite
- from micromagnetic calculation, Geophys. Res. Lett., 49, <u>e2022GL098437</u>, <u>https://</u>doi<u>.org/</u>10.1029/2022gl098437,
- 709 2022.
- Bärenstrauch, M., Vanhove, A. S., Allégra, S., Peuble, S., Gallice, F., Paran, F., Lavastre, V., and Girardot, F.:
- 711 Microbial diversity and geochemistry of groundwater impacted by steel slag leachates, Sci. Total Environ., 843,
- 712 156987, doi:10.1016/j.scitotenv.2022.156987, 2022.2022.
- Bartlett, K. B., Bartlett, D. S., Harriss, R. C., and Sebacher, D. I.: Methane emissions along a salt marsh salinity
- gradient, Biogeochemistry, 4, 183–202, doi:10.1007/BF02187365, 1987.
- Bazylinski, D. A., Frankel, R. B., Garratt-Reed, A. J., and Mann, S.: Biomineralization of iron sulfides Iron
- Sulfides in magnetotactic bacteria Magnetotactic Bacteria from sulfidic environments Sulfidic Environments, in: Iron
- Biominerals, edited by: Frankel, R. B. and Blakemore, R. P., Springer US, Boston, MA, 239–255,
- 718 doi:10.1007/978 1 4615 3810 3 17, 1991.
- 719 Bazylinski, D. A., Williams, T. J., Lefèvre, C. T., Trubitsyn, D., Fang, J., Beveridge, T. J., Moskowitz, B. M.,
- Ward, B., Schübbe, S., Dubbels, B. L., and Simpson, B.: Magnetovibrio blakemorei gen. nov., sp. nov., a
- 721 magnetotactic bacterium (Alphaproteobacteria: Rhodospirillaceae) isolated from a salt marsh, Int. J. Syst. Evol.
- 722 Microbiol., 63, 1824–1833, doi:10.1099/ijs.0.044453-0, 2013.
- 723 Benner, S. G., Hansel, C. M., Wielinga, B. W., Barber, T. M., and Fendorf, S.: Reductive dissolution and
- biomineralization of iron hydroxide under dynamic flow conditions, Environ. Sci. Technol., 36, 1705–1711,
- 725 doi:10.1021/es0156441, 2002.
- Blakemore, R.: Magnetotactic bacteria, Science, 190, 377–379, doi:10.1126/science.170679, 1975.
- Bolyen, E., Rideout, J. R., Dillon, M. R., Bokulich, N. A., Abnet, C. C., Al-Ghalith, G. A., Alexander, H., Alm,
- E. J., Arumugam, M., Asnicar, F., Bai, Y., Bisanz, J. E., Bittinger, K., Brejnrod, A., Brislawn, C. J., Brown, C.
- T., Callahan, B. J., Caraballo-Rodríguez, A. M., Chase, J., Cope, E. K., Da Silva, R., Diener, C., Dorrestein, P.

- C., Douglas, G. M., Durall, D. M., Duvallet, C., Edwardson, C. F., Ernst, M., Estaki, M., Fouquier, J., Gauglitz, J.
- 731 M., Gibbons, S. M., Gibson, D. L., Gonzalez, A., Gorlick, K., Guo, J., Hillmann, B., Holmes, S., Holste, H.,
- Huttenhower, C., Huttley, G. A., Janssen, S., Jarmusch, A. K., Jiang, L., Kaehler, B. D., Kang, K. B., Keefe, C.
- R., Keim, P., Kelley, S. T., Knights, D., Koester, I., Kosciolek, T., Kreps, J., Langille, M. G. I., Lee, J., Ley, R.,
- Liu, Y.-X., Loftfield, E., Lozupone, C., Maher, M., Marotz, C., Martin, B. D., McDonald, D., McIver, L. J.,
- 735 Melnik, A. V., Metcalf, J. L., Morgan, S. C., Morton, J. T., Naimey, A. T., Navas-Molina, J. A., Nothias, L. F.,
- Orchanian, S. B., Pearson, T., Peoples, S. L., Petras, D., Preuss, M. L., Pruesse, E., Rasmussen, L. B., Rivers, A.,
- Robeson, M. S., 2nd, Rosenthal, P., Segata, N., Shaffer, M., Shiffer, A., Sinha, R., Song, S. J., Spear, J. R.,
- 738 Swafford, A. D., Thompson, L. R., Torres, P. J., Trinh, P., Tripathi, A., Turnbaugh, P. J., Ul-Hasan, S., van der
- Hooft, J. J. J., Vargas, F., Vázquez-Baeza, Y., Vogtmann, E., von Hippel, M., et al.: Author Correction:
- 740 Reproducible, interactive, scalable and extensible microbiome data science using QIIME 2, Nat. Biotechnol., 37,
- 741 1091<del>, doi:10.1038/s41587-019-0252-6</del>, 2019.
- Bond, D. R. and Lovley, D. R.: Reduction of Fe(III) oxide by methanogens in the presence and absence of
- 743 extracellular quinones, Environ. Microbiol., 4, 115–124, doi:10.1046/j.1462-2920.2002.00279.x, 2002.2002.
- 744 Borrel, G., Adam, P. S., and Gribaldo, S.: Methanogenesis and the Wood-Ljungdahl pathway: An ancient, versatile, and fragile
- 745 association, Genome Biol. Evol., 8, 1706 1711, doi:10.1093/gbe/evw114, 2016.
- 746 Bovio-Winkler, P., Cabezas, A., and Etchebehere, C.: Database mining to unravel the ecology of the phylum
- Chloroflexi in methanogenic full scale bioreactors, Front. Microbiol., 11, 603234, doi:10.3389/fmicb.2020.603234,
- 748 2020.
- Brendel, P. J. and Luther, G. W.: Development of a Gold Amalgam Voltammetric Microelectrodegold amalgam
- 750 <u>voltammetric microelectrode</u> for the <u>Dd</u>etermination of <u>Dd</u>issolved Fe, Mn, O2, and S(-II) in <u>Pp</u>orewaters of
- 751 Marine and Freshwater Sediments freshwater sediments, Environ. Sci. Technol., 29, 751–761,
- 752 doi:10.1021/es00003a024, 1995.
- Bridgham, S. D., Megonigal, J. P., Keller, J. K., Bliss, N. B., and Trettin, C.: The carbon balance of North
- American wetlands, Wetlands, 26, 889–916, doi:10.1672/0277-5212(2006)26[889:TCBONA]2.0.CO;2, 2006.2006.
- Buckley, D. H., Baumgartner, L. K., and Visscher, P. T.: Vertical distribution of methane metabolism in
- microbial mats of the Great Sippewissett Salt Marsh, Environ. Microbiol., 10, 967–977, doi:10.1111/j.1462-
- 757 <del>2920.2007.01517.x,</del> 2008.
- 758 Cai, C., Leu, A. O., Xie, G.-J., Guo, J., Feng, Y., Zhao, J.-X., Tyson, G. W., Yuan, Z., and Hu, S.: A
- methanotrophic archaeon couples anaerobic oxidation of methane to Fe(III) reduction, ISME J., 12, 1929–1939,
- 760 doi:10.1038/s41396 018 0109 x, 2018.
- 761 Cai, M., Yin, X., Tang, X., Zhang, C., Zheng, Q., and Li, M.: Metatranscriptomics reveals different features of
- methanogenic archaea among global vegetated coastal ecosystems, Sci. Total Environ., 802, 149848,
- 763 doi:10.1016/j.scitotenv.2021.149848, 2022.2022.
- Callahan, B. J., McMurdie, P. J., Rosen, M. J., Han, A. W., Johnson, A. J. A., and Holmes, S. P.: DADA2: High-
- resolution sample inference from Illumina amplicon data, Nat. Methods, 13, 581–583, doi:10.1038/nmeth.3869,
- 766 2016.

- 767 Carrión, O., Pratscher, J., Richa, K., Rostant, W. G., Farhan Ul Haque, M., Murrell, J. C., and Todd, J. D.:
- Methanethiol and dimethylsulfide cycling in stiffkey saltmarsh, Front. Microbiol., 10, 1040,
- 769 doi:10.3389/fmicb.2019.01040, 2019.
- Cavalieri, A. J. and Huang, A. H. C.: Accumulation of proline and glycinebetaine in Spartina alterniflora Loisel.
- in response to NaCl and nitrogen in the marsh, Oecologia, 49, 224–228, doi:10.1007/BF00349192, 1981.
- 772 Chmura, G. L., Kellman, L., and Guntenspergen, G. R.: The greenhouse gas flux and potential global warming
- feedbacks of a northern macrotidal and microtidal salt marsh, Environ. Res. Lett., 6, 044016, doi:10.1088/1748
- 774 <del>9326/6/4/044016,</del> 2011.
- Coleman, M. L., Hedrick, D. B., Lovley, D. R., White, D. C., and Pye, K.: Reduction of Fe(III) in sediments by
- sulphate-reducing bacteria, Nature, 361, 436–438, 1993.
- 777 Cruz Viggi, C., Rossetti, S., Fazi, S., Paiano, P., Majone, M., and Aulenta, F.: Magnetite particles triggering a
- faster and more robust syntrophic pathway of methanogenic propionate degradation, Environ. Sci. Technol., 48,
- 779 7536–7543, doi:10.1021/es5016789, 2014.
- Day, L. A., Kelsey, E. L., Fonseca, D. R., and Costa, K. C.: Interspecies Formate Exchange Drives Syntrophic
- Growth of Syntrophotalea carbinolica and Methanococcus maripaludis, Appl. Environ. Microbiol., 88, e0115922,
- 782 doi:10.1128/aem.01159-22, 2022.
- 783 De Cáceres, M., Legendre, P., and Moretti, M.: Improving indicator species analysis by combining groups of
- 784 sites, Oikos, 119, 1674–1684, doi:10.1111/j.1600.0706.2010.18334.x, 2010.2010.
- De Cáceres, M., Legendre, P., and Wiser, S. K., and Brotons, L.: Using species combinations in indicator value
- analyses, Methods Ecol. Evol., in Ecology and Evolution, 3, 973–982, https://doi:.org/10.1111/j.2041-
- 787 210X.2012.00246.x, 2012.
- 788 Demitrack, A.: A Search for Bacterial Magnetite in the Sediments of Eel Marsh, Woods Hole, Massachusetts, in:
- 789 Magnetite Biomineralization and Magnetoreception in Organisms: A New Biomagnetism, edited by: Kirschvink,
- J. L., Jones, D. S., and MacFadden, B. J., Springer US, Boston, MA, 625–645, doi:10.1007/978 1 4613 0313 8 35,
- 791 1985.
- Deng, P., Wang, L., Li, X., Zhang, J., and Jiang, H.: Geobacter grbiciae—A new electron donor in the formation
- of co-cultures via direct interspecies electron transfer, Microbiol. Res. (Pavia), 14, 1774–1787,
- 794 doi:10.3390/microbiolres14040122, 2023.
- 795 Deévai, I. and DeLlaune, R.D.: Formation of volatile sulfur compounds in salt marsh sediment as influenced by
- 796 soil redox condition, Org. Geochem., Organic Geochemistry, 23, 283–287, doi:10.1016/0146-6380(95)00024-9, 1995.
- Dewitt, P. and Daiber, F. C.: The hydrography of the Broadkill River estuary, Delaware, Chesapeake Science, 14,
- 798 28–40, doi:10.2307/1350700, 1973.
- 799 Delaware Water Quality Portal Station BR40: https://cema.udel.edu/applications/waterquality/, last access: 13 June 2024.
- Du, J., Yin, Q., Gu, M., and Wu, G.: New insights into the effect of ethanol and volatile fatty acids proportions on
- methanogenic activities and pathways, Environ. Res., 194, 110644, 2021.

- Dunlop, D. J.: Superparamagnetic and single-domain threshold sizes in magnetite, J. Geophys. Res., 78, 1780–
- 803 1793, doi:10.1029/jb078i011p01780, 1973.
- 804 Dunlop, D. J. and Ozdemir, O.: Cambridge studies in magnetism: Rock magnetism: Fundamentals and frontiers
- series number 3: Fundamentals and frontiers, Cambridge University Press, Cambridge, England, 596 pp.,
- https://doi<sub>\*.</sub>org/10.1017/cbo9780511612794<sub>-</sub>,+2001., 2011.
- Dyksma, S., Lenk, S., Sawicka, J. E., and Mußmann, M.: Uncultured Gammaproteobacteria and
- Desulfobacteraceae account for major acetate assimilation in a coastal marine sediment, Front. Microbiol., 9,
- 809 3124, doi:10.3389/fmicb.2018.03124, 2018.
- 810 Egli, R.: Characterization of Individual Rock Magnetic Components individual rock magnetic components by
- 811 Aanalysis of Remanence Curves remanence curves, 1. Unmixing natural sediments, Stud. Geophys. Natural
- 812 Sediments, Studia Geophysica et Geodaetica, 48, 391–446, Geod.,
- https://doi+.org/10.1023/B:SGEG.0000020839.45304.6d, 2004.
- 814 Eichler, B. and Schink, B.: Fermentation of primary alcohols and diols and pure culture of syntrophically alcohol-
- \$15 oxidizing anaerobes, Arch. Microbiol., 143, 60–66, doi:10.1007/bf00414769, 1985.
- 816 Enkin, R. J. and Dunlop, D. J.: A micromagnetic study of pseudo single-domain remanence in magnetite, J.
- 817 Geophys. Res., 92, 12726, doi:10.1029/jb092ib12p12726, 1987.
- 818 Ettwig, K. F., Zhu, B., Speth, D., Keltjens, J. T., Jetten, M. S. M., and Kartal, B.: Archaea catalyze iron-
- dependent anaerobic oxidation of methane, Proc. Natl. Acad. Sci. U. S. A., 113, 12792–12796,
- 820 doi:10.1073/pnas.1609534113, 2016.
- 821 Evans, P. N., Parks, D. H., Chadwick, G. L., Robbins, S. J., Orphan, V. J., Golding, S. D., and Tyson, G. W.:
- Methane metabolism in the archaeal phylum Bathyarchaeota revealed by genome-centric metagenomics, Science,
- 823 350, 434–438, doi:10.1126/science.aac7745, 2015.
- 824 Evans, P. N., Boyd, J. A., Leu, A. O., Woodcroft, B. J., Parks, D. H., Hugenholtz, P., and Tyson, G. W.: An
- evolving view of methane metabolism in the Archaea, Nat. Rev. Microbiol., 17, 219–232, doi:10.1038/s41579\_018
- 826 <del>0136 7,</del> 2019.
- Farag, I. F., Biddle, J. F., Zhao, R., Martino, A. J., House, C. H., and León-Zayas, R. I.: Metabolic potentials of
- archaeal lineages resolved from metagenomes of deep Costa Rica sediments, ISME J., 14, 1345–1358, 2020.
- Fillol, M., Auguet, J.-C., Casamayor, E. O., and Borrego, C. M.: Insights in the ecology and evolutionary history
- of the Miscellaneous Crenarchaeotic Group lineage, ISME J., 10, <del>1-13, doi:10.1038/ismej.2015.143, 2015</del>665–677,
- 831 <u>2016</u>.
- Fitzsimons, M. F., Jemmett, A. W., and Wolff, G. A.: A preliminary study of the geochemistry of methylamines
- in a salt marsh, Org. Geochem., 27, 15–24, doi:10.1016/S0146-6380(97)00062-4, 1997.
- Franklin, M. J., Wiebe, W. J., and Whitman, W. B.: Populations of methanogenic bacteria in a georgia salt marsh,
- 835 Appl. Environ. Microbiol., 54, 1151–1157, doi:10.1128/aem.54.5.1151-1157.1988, 1988.1988.

- Fu, L., Zhou, T., Wang, J., You, L., Lu, Y., Yu, L., and Zhou, S.: NanoFe3O4 as solid electron shuttles to
- 837 accelerate acetotrophic methanogenesis by Methanosarcina barkeri, Front. Microbiol., 10, 388,
- 838 doi:10.3389/fmicb.2019.00388, 2019.
- 639 Garber, A. I., Nealson, K. H., and Merino, N.: Large-scale prediction of outer-membrane multiheme cytochromes
- uncovers hidden diversity of electroactive bacteria and underlying pathways, Front. Microbiol., 15, 1448685,
- 841 doi:10.3389/fmicb.2024.1448685, 2024.
- 642 Gibb, S. W., Mantoura, R. F. C., and Liss, P. S.: Ocean-atmosphere exchange and atmospheric speciation of
- ammonia and methylamines in the region of the NW Arabian Sea, Global Biogeochem. Cycles, 13, 161–178,
- 844 doi:10.1029/98gb00743, 1999.
- 645 Glob, E. and Sørensen, J.: Determination of dissolved and exchangeable trimethylamine pools in sediments,
- Journal of Microbiological Methods, 6, 347–355, 1987.
- Gordon, A., Plessy, C., and K., S.: fastx toolkit: FASTA/FASTQ pre-processing programs, Github, 2010.
- 648 Gribsholt, B., Kostka, J. E., and Kristensen, E.: Impact of fiddler crabs and plant roots on sediment
- biogeochemistry in a Georgia saltmarsh, Mar. Ecol. Prog. Ser., 259, 237–251, doi:10.3354/meps259237, 2003.
- Guider, J. T., Yoshimura, K. M., Block, K. R., Biddle, J. F., and Shah Walter, S. R.: Archaeal blooms and busts
- in an estuarine time series, Environ. Microbiol., 26, e16584, doi:10.1111/1462 2920.16584, 2024.
- Hackmann, T. J.: The vast landscape of carbohydrate fermentation in prokaryotes, FEMS Microbiol. Rev., 48, fuae016,
- 853 doi:10.1093/femsre/fuae016, 2024.
- Hall, N., Wong, W. W., Lappan, R., Ricci, F., Glud, R. N., Kawaichi, S., Rotaru, A.-E., Greening, C., and Cook,
- P. L. M.: Aerotolerant methanogens use seaweed and seagrass metabolites to drive marine methane emissions,
- bioRxiv, <a href="https://doi+.org/10.1101/2024.10.14.618369">https://doi+.org/10.1101/2024.10.14.618369</a>, 2024.
- Hansel, C. M., Benner, S. G., Neiss, J., Dohnalkova, A., Kukkadapu, R. K., and Fendorf, S.: Secondary
- 858 mineralization pathways induced by dissimilatory iron reduction of ferrihydrite under advective flow, Geochim.
- 859 Cosmochim. Acta, 67, 2977–2992<del>, doi:10.1016/s0016-7037(03)00276-x</del>, 2003.
- Hartman, W. H., Bueno de Mesquita, C. P., Theroux, S. M., Morgan-Lang, C., Baldocchi, D. D., and Tringe, S.
- 61 G.: Multiple microbial guilds mediate soil methane cycling along a wetland salinity gradient, mSystems, 9,
- 862 <del>e0093623, doi:10.1128/msystems.00936-</del>e00936-23, 2024.
- Herbold, C. W., Pelikan, C., Kuzyk, O., Hausmann, B., Angel, R., Berry, D., and Loy, A.: A flexible and
- 864 economical barcoding approach for highly multiplexed amplicon sequencing of diverse target genes, Front.
- Microbiol., 6, 731, doi:10.3389/fmicb.2015.00731, 2015.
- 866 Heywood, B. R., Bazylinski, D. A., Garratt Reed, A., Mann, S., and Frankel, R. B.: Controlled biosynthesis of greigite
- 867 (Fe3S4) in magnetotactic bacteria, Sei. Nat., 77, 536–538, doi:10.1007/bf01139266, 1990.
- Holmes, D. E., Shrestha, P. M., Walker, D. J. F., Dang, Y., Nevin, K. P., Woodard, T. L., and Lovley, D. R.:
- Metatranscriptomic evidence for direct interspecies electron transfer between Geobacter and Methanothrix

- species in methanogenic rice paddy soils, Appl. Environ. Microbiol., 83, e00223 17,
- 871 <a href="https://doi:.org/10.1128/aemAEM">https://doi:.org/10.1128/aemAEM</a>.00223-17, 2017.
- Holmquist, J. R., Eagle, M., Molinari, R. L., Nick, S. K., Stachowicz, L. C., and Kroeger, K. D.: Mapping
- methane reduction potential of tidal wetland restoration in the United States, Communications Earth &
- 874 Environment, 4, 1–11, doi:10.1038/s43247-023-00988-y, 2023.
- Hou, J., Wang, Y., Zhu, P., Yang, N., Liang, L., Yu, T., Niu, M., Konhauser, K., Woodcroft, B. J., and Wang, F.:
- Taxonomic and carbon metabolic diversification of Bathyarchaeia during its coevolution history with early Earth
- surface environment, Sci. Adv., 9, eadf5069, doi:10.1126/sciadv.adf5069, 2023.
- Howarth, R. W.: The ecological significance of sulfur in the energy dynamics of salt marsh and coastal marine
- 879 sediments, Biogeochemistry, 1, 5–27, doi:10.1007/bf02181118, 1984.
- Howarth, R. W. and Giblin, A.: Sulfate reduction in the salt marshes at Sapelo Island, Georgia, Limnol.
- 881 Oceanogr., 28, 70–82, doi:10.4319/lo.1983.28.1.0070, 1983.
- Howarth, R. W. and Teal, J. M.: Sulfate reduction in a New England salt marsh, Limnol. Oceanogr., 24, 999–
- 883 1013, doi:10.4319/lo.1979.24.6.0999, 1979.
- Hyun, J.-H., Smith, A. C., and Kostka, J. E.: Relative contributions of sulfate- and iron(III) reduction to organic
- matter mineralization and process controls in contrasting habitats of the Georgia saltmarsh, Appl. Geochem., 22,
- 886 2637–2651, doi:10.1016/j.apgeochem.2007.06.005, 2007.2007.
- Jackson, M. and Solheid, P.: On the quantitative analysis and evaluation of magnetic hysteresis data:
- HYSTERESIS LOOP EVALUATION AND ANALYSIS, Geochem. Geophys. Geosyst., 11, Q04Z15,
- 889 doi:10.1029/2009gc002932, 2010.
- Jameson, E., Stephenson, J., Jones, H., Millard, A., Kaster, A.-K., Purdy, K. J., Airs, R., Murrell, J. C., and Chen,
- 891 Y.: Deltaproteobacteria (Pelobacter) and Methanococcoides are responsible for choline-dependent
- methanogenesis in a coastal saltmarsh sediment, ISME J., 13, 277–289, doi:10.1038/s41396-018-0269-8, 2019.
- Jones, H. J., Kröber, E., Stephenson, J., Mausz, M. A., Jameson, E., Millard, A., Purdy, K. J., and Chen, Y.: A
- new family of uncultivated bacteria involved in methanogenesis from the ubiquitous osmolyte glycine betaine in
- 895 coastal saltmarsh sediments, Microbiome, 7, 120, doi:10.1186/s40168 019 0732 4, 2019.
- Jørgensen, B. B.: Bacteria and Marine Biogeochemistry, in: Marine Geochemistry, edited by: Schulz, H. D. and
- Zabel, M., Springer Berlin Heidelberg, Berlin, Heidelberg, 169–206, doi:10.1007/3-540-32144-6-5, 2006.
- 898 Jørgensen, B. B. and Kasten, S.: Sulfur Cycling and Methane Oxidation, in: Marine Geochemistry, edited by:
- Schulz, H. D. and Zabel, M., Springer Berlin Heidelberg, Berlin, Heidelberg, 271–309, doi:10.1007/3-540-32144
- 900 <del>6 8,</del> 2006.
- Jussofie, A. and Gottschalk, G.: Further studies on the distribution of cytochromes in methanogenic bacteria,
- 902 FEMS Microbiol. Lett., 37, 15–18, doi:10.1111/j.1574-6968.1986.tb01758.x, 1986.1986.
- Kappler, A., Bryce, C., Mansor, M., Lueder, U., Byrne, J. M., and Swanner, E. D.: An evolving view on

- biogeochemical cycling of iron, Nat. Rev. Microbiol., 19, 360–374, doi:10.1038/s41579\_020\_00502\_7, 2021.
- 805 Kappler, A., Thompson, A., and Mansor, M.: Impact of biogenic magnetite formation and transformation on
- biogeochemical cycles, Elements <u>(Que.)</u>, 19, 222–227, doi:10.2138/gselements.19.4.222, 2023.
- Kato, S., Hashimoto, K., and Watanabe, K.: Methanogenesis facilitated by electric syntrophy via
- 908 (semi)conductive iron-oxide minerals, Environ. Microbiol., 14, 1646–1654, doi:10.1111/j.1462 2920.2011.02611.x,
- 909 <del>2012.</del>2012.
- Kiene, R. P. and Visscher, P. T.: Production and fate of methylated sulfur compounds from methionine and
- 911 dimethylsulfoniopropionate in anoxic salt marsh sediments, Appl. Environ. Microbiol., 53, 2426–2434,
- 912 doi:10.1128/aem.53.10.2426-2434.1987, 1987.1987.
- 913 King, G. M.: Distribution and Metabolism of Quaternary Amines in Marine Sediments, in: Nitrogen Cycling in Coastal Marine
- 914 Environments, edited by: Blackburn, T. H. and Sorensen, J., John Wiley and Sons (WIE), New York, NY, 143-173, 1988.
- King, G. M.: Methanogenesis from methylated amines in a hypersaline algal mat, Appl. Environ. Microbiol., 54,
- 916 130–136, 1988.
- Koblitz, J., Halama, P., Spring, S., Thiel, V., Baschien, C., Hahnke, R. L., Pester, M., Overmann, J., and Reimer,
- 918 L. C.: MediaDive: the expert-curated cultivation media database, Nucleic Acids Res., 51, D1531–D1538,
- 919 doi:10.1093/nar/gkac803, 2023.
- 920 Kolinko, S., Richter, M., Glöckner, F.-O., Brachmann, A., and Schüler, D.: Single-cell genomics of uncultivated
- deep-branching magnetotactic bacteria reveals a conserved set of magnetosome genes: Genomic analysis of an
- uncultivated multicellular magnetotactic prokaryote, Environ. Microbiol., 18, 21–37, doi:10.1111/1462-2920.12907,
- 923 2016.
- Koretsky, C. M., Moore, C. M., Lowe, K. L., Meile, C., DiChristina, T. J., and Van Cappellen, P.: Seasonal
- oscillation of microbial iron and sulfate reduction in saltmarsh sediments (Sapelo Island, GA, USA),
- Biogeochemistry, 64, 179–203, doi:10.1023/a:1024940132078, 2003.
- 827 Koretsky, C. M., Van Cappellen, P., DiChristina, T. J., Kostka, J. E., Lowe, K. L., Moore, C. M., Roychoudhury,
- A. N., and Viollier, E.: Salt marsh pore water geochemistry does not correlate with microbial community
- 929 structure, Estuar. Coast. Shelf Sci., 62, 233–251, doi:10.1016/j.ecss.2004.09.001, 2005.
- Kostka, J. E. and Luther, G. W.: Partitioning and speciation of solid phase iron in saltmarsh sediments, Geochim.
- 931 Cosmochim. Acta, 58, 1701–1710, doi:10.1016/0016-7037(94)90531-2, 1994.
- Kostka, J. E. and Luther, G. W.: Seasonal cycling of Fe in saltmarsh sediments, Biogeochemistry, 29, 159–181,
- 933 doi:10.1007/BF00000230, 1995.
- Kostka, J. E., Roychoudhury, A., and Van Cappellen, P.: Rates and controls of anaerobic microbial respiration
- across spatial and temporal gradients in saltmarsh sediments, Biogeochemistry, 60, 49–76,
- 936 doi:10.1023/A:1016525216426, 2002a.
- Kostka, J. E., Gribsholt, B., Petrie, E., Dalton, D., Skelton, H., and Kristensen, E.: The rates and pathways of
- carbon oxidation in bioturbated saltmarsh sediments, Limnol. Oceanogr., 47, 230–240,

- 939 doi:10.4319/lo.2002.47.1.0230, 2002b.
- Krause, S. J., Liu, J., Yousavich, D. J., Robinson, D., Hoyt, D. W., Qin, Q., and Treude: Evidence of cryptic
- methane cycling and non-methanogenic methylamine consumption in the sulfate-reducing zone of sediment in
- the Santa Barbara Basin, California, Biogeosciences, 20, 4377–4390, 2023.
- 943 Krause, S. J. E. and Treude, T.: Deciphering cryptic methane cycling: Coupling of methylotrophic
- methanogenesis and anaerobic oxidation of methane in hypersaline coastal wetland sediment, Geochim.
- 945 Cosmochim. Acta, 302, 160–174, doi:10.1016/j.gca.2021.03.021, 2021.
- Krause, S. J. E., Wipfler, R., Liu, J., Yousavich, D. J., Robinson, D., Hoyt, D. W., Qin, Q., Wenzhöfer, Orphan, V. J.
- 947 F., Janssen, F., Valentine, D. L., and Treude, T.: Evidence Spatial evidence of cryptic methane cycling and non-
- 948 methanogenic methylamine consumption methylotrophic metabolisms along a land-ocean transect in the sulfate-
- 949 reducing zone of salt marsh sediment in the Santa Barbara Basin, California, Biogeosciences, 20, 4377-4390, Geochim.
- 950 Cosmochim. Acta, https://doi:.org/10.5194/bg-20-4377-2023, 20231016/j.gca.2025.07.019, 2025.
- 951 Kreisler, J. and Slotznick, S. P.: Magnetite Preservation and Diagenesis in Marine Sediments, Geophys. Res. Lett., in revision
- 952 Lee, C. and Olson, B. L.: Dissolved, exchangeable and bound aliphatic amines in marine sediments: initial
- ps3 results, Org. Geochem., Organic Geochemistry, 6, 259–263, doi:10.1016/0146-6380(84)90047-0, 1984.
- L'Haridon, S., Chalopin, M., Colombo, D., and Toffin, L.: Methanococcoides vulcani sp. nov., a marine
- methylotrophic methanogen that uses betaine, choline and N,N-dimethylethanolamine for methanogenesis,
- isolated from a mud volcano, and emended description of the genus Methanococcoides, Int. J. Syst. Evol.
- 957 Microbiol., 64, 1978–1983<del>, doi:10.1099/ijs.0.058289-0</del>, 2014.
- Liang, B., Wang, L.-Y., Mbadinga, S. M., Liu, J.-F., Yang, S.-Z., Gu, J.-D., and Mu, B.-Z.: Anaerolineaceae and
- 959 Methanosaeta turned to be the dominant microorganisms in alkanes-dependent methanogenic culture after long-
- 960 term of incubation, AMB Express, 5, 117, doi:10.1186/s13568-015-0117-4, 2015.
- Liang, L., Sun, Y., Dong, Y., Ahmad, T., Chen, Y., Wang, J., and Wang, F.: Methanococcoides orientis sp. nov.,
- a methylotrophic methanogen isolated from sediment of the East China Sea, Int. J. Syst. Evol. Microbiol., 72,
- 963 05384, https://doi:.org/10.1099/ijsem.0.005384, 2022.
- Lin, W., Zhang, W., Zhao, X., Roberts, A. P., Paterson, G. A., Bazylinski, D. A., and Pan, Y.: Genomic
- 965 expansion of magnetotactic bacteria reveals an early common origin of magnetotaxis with lineage-specific
- 966 evolution, ISME J., 12, 1508–1519, 2018.
- Liu, F., Rotaru, A.-E., Shrestha, P. M., Malvankar, N. S., Nevin, K. P., and Lovley, D. R.: Magnetite
- compensates for the lack of a pilin-associated c-type cytochrome in extracellular electron exchange: Magnetite
- 969 compensates for the lack of OmcS, Environ. Microbiol., 17, 648–655<del>, doi:10.1111/1462-2920.12485</del>, 2015.
- Liu, J., Klonicki-Ference, E., Krause, S. J. E., and Treude, T.: Iron oxides fuel anaerobic oxidation of methane in
- the presence of sulfate in hypersaline coastal wetland sediment, Environ. Sci. Technol., 59, 513–522, 2025.
- Li, Y., Wang, S., Ji, B., Yuan, Q., Wei, S., Lai, Q., Wu, K., Jiang, L., and Shao, Z.: Sulfurovum mangrovi sp.
- 973 nov., an obligately chemolithoautotrophic, hydrogen-oxidizing bacterium isolated from coastal marine sediments,
- 974 Int. J. Syst. Evol. Microbiol., 73, 006142, https://doi.org/10.1099/ijsem.0.006142, 2023.

- Lomans, B. P., van der Drift, C., Pol, A., and Op den Camp, H. J. M.: Microbial cycling of volatile organic sulfur
- 976 compounds, Cell. Mol. Life Sci., 59, 575–588, doi:10.1007/s00018-002-8450-6, 2002.
- Lovley, D. R.: Happy together: microbial communities that hook up to swap electrons, ISME J., 11, 327–336,
- 978 doi:10.1038/ismej.2016.136, 2017a.
- Lovley, D. R.: Syntrophy Goes Electric: Direct Interspecies Electron Transfer, Annu. Rev. Microbiol., 71, 643–
- 980 664, doi:10.1146/annurev micro 030117 020420, 2017b.
- Lovley, D. R. and Holmes, D. E.: Electromicrobiology: the ecophysiology of phylogenetically diverse
- 982 electroactive microorganisms, Nat. Rev. Microbiol., 20, 5–19, doi:10.1038/s41579-021-00597-6, 2022.
- Lovley, D. R., Roden, E. E., Phillips, E. J. P., and Woodward, J. C.: Enzymatic iron and uranium reduction by
- 984 <u>sulfate-reducing bacteria, Mar. Geol., 113, 41–53, 1993.</u>
- 985 Lowe, K. L., Dichristina, T. J., Roychoudhury, A. N., and Van Cappellen, P.: Microbiological and Geochemical
- P86 Characterization of Microbial Fe(III) Reduction in Salt Marsh Sediments, Geomicrobiol. J., 17, 163–178,
- 987 doi:10.1080/01490450050023836, 2000.
- Luther, G. W., III, Glazer, B. T., Ma, S., Trouwborst, R. E., Moore, T. S., Metzger, E., Kraiya, C., Waite, T. J.,
- Druschel, G., Sundby, B., Taillefert, M., Nuzzio, D. B., Shank, T. M., Lewis, B. L., and Brendel, P. J.: Use of
- 990 voltammetric solid-state (micro)electrodes for studying biogeochemical processes: Laboratory measurements to
- real time measurements with an in situ electrochemical analyzer (ISEA), Mar. Chem., 108, 221–235,
- 992 doi:10.1016/j.marchem.2007.03.002, 2008.
- 993 Määttä, T. and Malhotra, A.: The hidden roots of wetland methane emissions, Glob. Chang. Biol., 30, e17127,
- 994 doi:10.1111/geb.17127, 2024.
- Matheus Carnevali, P. B., Schulz, F., Castelle, C. J., Kantor, R. S., Shih, P. M., Sharon, I., Santini, J. M., Olm, M.
- 996 R., Amano, Y., Thomas, B. C., Anantharaman, K., Burstein, D., Becraft, E. D., Stepanauskas, R., Woyke, T., and
- Banfield, J. F.: Hydrogen-based metabolism as an ancestral trait in lineages sibling to the Cyanobacteria, Nat.
- 998 Commun., 10, 463<del>, doi:10.1038/s41467-018-08246-y</del>, 2019.
- Mausz, M. A. and Chen, Y.: Microbiology and ecology of methylated Amine metabolism in marine ecosystems,
- 1000 <u>Curr. Issues Mol. Biol., 33, 133–148, 2019.</u>
- Maxbauer, D. P., Feinberg, J. M., and Fox, D. L.: MAX UnMix: A web application for unmixing magnetic
- 1002 coercivity distributions, Comput. Geosci., 95, 140–145, doi:10.1016/j.cageo.2016.07.009, 2016.
- McIlroy, S. J., Kirkegaard, R. H., Dueholm, M. S., Fernando, E., Karst, S. M., Albertsen, M., and Nielsen, P. H.:
- 1004 Culture-independent analyses reveal novel Anaerolineaceae as abundant primary fermenters in anaerobic
- digesters treating waste activated sludge, Front. Microbiol., 8, 1134, doi:10.3389/fmieb.2017.01134, 2017.
- 1006 Moore, R.: Feature Table -- R6 and s3 classes for feature tables, data, and microbiome analysis, Github, 2020.
- Mulholland, M. M. and Otte, M. L.: The effects of nitrogen supply and salinity on DMSP, glycine betaine and
- proline concentrations in leaves of Spartina anglica, Aquat. Bot., 72, 193–200, doi:10.1016/s0304.3770(01)00228.5,

- 1009 2002.
- 1010 Munson, M. A., Nedwell, D. B., and Embley, T. M.: Phylogenetic diversity of Archaea in sediment samples from
- 1011 a coastal salt marsh, Appl. Environ. Microbiol., 63, 4729–4733, doi:10.1128/aem.63.12.4729-4733.1997, 1997.1997.
- Nobu, M. K., Narihiro, T., Kuroda, K., Mei, R., and Liu, W.-T.: Chasing the elusive Euryarchaeota class WSA2:
- genomes reveal a uniquely fastidious methyl-reducing methanogen, ISME J., 10, 2478–2487,
- 1014 doi:10.1038/ismej.2016.33, 2016.
- Oremland, R. S. and Polcin, S.: Methanogenesis and sulfate reduction: competitive and noncompetitive substrates
- 1016 in estuarine sediments, Appl. Environ. Microbiol., 44, 1270–1276, doi:10.1128/aem.44.6.1270-1276.1982,
- 1017 <del>1982.</del><u>1982.</u>
- Oremland, R. S., Marsh, L. M., and Polcin, S.: Methane production and simultaneous sulphate reduction in
- 1019 anoxic, salt marsh sediments, Nature, 296, 143–145, doi:10.1038/296143a0, 1982.
- Parada, A. E., Needham, D. M., and Fuhrman, J. A.: Every base matters: assessing small subunit rRNA primers
- for marine microbiomes with mock communities, time series and global field samples, Environ. Microbiol., 18,
- 1022 1403–1414, doi:10.1111/1462-2920.13023, 2016.
- Parkes, R. J., Brock, F., Banning, N., Hornibrook, E. R. C., Roussel, E. G., Weightman, A. J., and Fry, J. C.:
- 1024 <u>Changes in methanogenic substrate utilization and communities with depth in a salt-marsh, creek sediment in </u>
- southern England, Estuar. Coast. Shelf Sci., 96, 170–178, 2012a.
- Parkes, R. J., Brock, F., Banning, N., Hornibrook, E. R. C., Roussel, E. G., Weightman, A. J., and Fry, J. C.:
- 1027 Changes in methanogenic substrate utilization and communities with depth in a salt-marsh, creek sediment in
- 1028 southern England, Estuar. Coast. Shelf Sci., 96, 170–178, doi:10.1016/j.ecss.2011.10.025, 20122012b.
- Perez-Molphe-Montoya, E., Küsel, K., and Overholt, W. A.: Redefining the phylogenetic and metabolic diversity
- 1030 of phylum Omnitrophota, Environ. Microbiol., 24, 5437–5449, doi:10.1111/1462\_2920.16170, 2022.
- 1031 Peters, C. and Dekkers, M. J.: Selected room temperature magnetic parameters as a function of mineralogy,
- 1032 concentration and grain size, Phys. Chem. Earth (2002), 28, 659–667, doi:10.1016/s1474-7065(03)00120-7, 2003.
- Poffenbarger, H. J., Needelman, B. A., and Megonigal, J. P.: Salinity influence on methane emissions from tidal
- 1034 marshes, Wetlands, 31, 831–842, doi:10.1007/s13157-011-0197-0, 2011.
- Ravin, N. V., Muntyan, M. S., Smolyakov, D. D., Rudenko, T. S., Beletsky, A. V., Mardanov, A. V., and
- 1036 Grabovich, M. Y.: Metagenomics Revealed a New Genus "Candidatus Thiocaldithrix dubininis" gen. nov., sp.
- 1037 nov. and a New Species "Candidatus Thiothrix putei" sp. nov. in the Family Thiotrichaceae, Some Members of
- 1038 Which Have Traits of Both Na+- and H+-Motive Energetics, Int. J. Mol. Sci., 24, 14199.
- 1039 doi:10.3390/ijms241814199, 2023.
- Robeson, M. S., 2nd, O'Rourke, D. R., Kaehler, B. D., Ziemski, M., Dillon, M. R., Foster, J. T., and Bokulich, N.
- 1041 A.: RESCRIPt: Reproducible sequence taxonomy reference database management, PLoS Comput. Biol., 17,
- 1042 e1009581, doi:10.1371/journal.pcbi.1009581, 2021.

- Rosentreter, J. A., Borges, A. V., Deemer, B. R., Holgerson, M. A., Liu, S., Song, C., Melack, J., Raymond, P.
- 1044 A., Duarte, C. M., Allen, G. H., Olefeldt, D., Poulter, B., Battin, T. I., and Eyre, B. D.: Half of global methane
- emissions come from highly variable aquatic ecosystem sources, Nat. Geosci., 14, 225–230, doi:10.1038/s41561
- 1046 <del>021 00715 2</del>, 2021.
- Rotaru, A., Posth, N., Löscher, C., Miracle, M. R., Vincence, E., Cox, R. P., Thompson, J., Poulton, S., and
- 1048 Thamdrup, B.: Interspecies interactions mediated by conductive minerals in the sediments of the Iron rich
- 1049 Meromictic Lake La Cruz, Spain, Limnetica, 38, 21–40, doi:10.23818/LIMN.38.10, 2019.
- Rotaru, A.-E., Shrestha, P. M., Liu, F., Shrestha, M., Shrestha, D., Embree, M., Zengler, K., Wardman, C., Nevin,
- 1051 K. P., and Lovley, D. R.: A new model for electron flow during anaerobic digestion: direct interspecies electron
- transfer to Methanosaeta for the reduction of carbon dioxide to methane, Energy Environ. Sci., 7, 408–415,
- 1053 doi:10.1039/C3EE42189A, 2014a2014.
- 1054 Rotaru, A.-E., Shrestha, P. M., Liu, F., Markovaite, B., Chen, S., Nevin, K. P., and Lovley, D. R.: Direct interspecies electron
- 1055 transfer between Geobacter metallireducens and Methanosarcina barkeri, Appl. Environ. Microbiol., 80, 4599-4605,
- 1056 doi:10.1128/AEM.00895-14, 2014b.
- Rotaru, A.-E., Calabrese, F., Stryhanyuk, H., Musat, F., Shrestha, P. M., Weber, H. S., Snoeyenbos-West, O. L.
- O., Hall, P. O. J., Richnow, H. H., Musat, N., and Thamdrup, B.: Conductive Particles Enable Syntrophic Acetate
- Oxidation between Geobacter and Methanosarcina from Coastal Sediments, MBio, 9, 00226–00218,
- 1060 doi:10.1128/mBio.00226-18, 2018.
- Rotaru, A.-E., Yee, M. O., and Musat, F.: Microbes trading electricity in consortia of environmental and
- biotechnological significance, Curr. Opin. Biotechnol., 67, 119–129, doi:10.1016/j.copbio.2021.01.014, 2021.
- Ruiz-Blas, F., Bartholomäus, A., Yang, S., Wagner, D., Henny, C., Russell, J. M., Kallmeyer, J., and Vuillemin,
- 1064 A.: Metabolic features that select for Bathyarchaeia in modern ferruginous lacustrine subsurface sediments,
- 1065 ISME Commun., 4, ycae112, 2024.
- Saunders, N. F. W., Goodchild, A., Raftery, M., Guilhaus, M., Curmi, P. M. G., and Cavicchioli, R.: Predicted
- 1067 roles for hypothetical proteins in the low-temperature expressed proteome of the Antarctic archaeon
- 1068 Methanococcoides burtonii, J. Proteome Res., 4, 464–472, doi:10.1021/pr049797+, 2005.
- Saunois, M., Bousquet, P., Poulter, B., Peregon, A., and Ciais, P.: Global Methane Budget 2000-2012 (V.1.0,
- issued June 2016 and V.1.1, issued December 2016),
- 1071 https://doi<sub>\*.</sub>org/10.3334/CDIAC/GLOBAL METHANE BUDGET 2016 V1.1, 2016.
- Schink, B.: Fermentation of 2,3-butanediol by Pelobacter carbinolicus sp. nov. and Pelobacter propionicus sp.
- nov., and evidence for propionate formation from C2 compounds, Arch. Microbiol., 137, 33–41,
- 1074 doi:10.1007/bf00425804, 1984.
- Schink, B.: Energetics of syntrophic cooperation in methanogenic degradation, Microbiol. Mol. Biol. Rev., 61,
- 1076 262–280, doi:10.1128/mmbr.61.2.262 280.1997, 1997.1997.
- Schink, B.: The Genus Pelobacter, in: The Prokaryotes, Springer New York, New York, NY, 5–11, doi:10.1007/0-
- 1078 <del>387-30747-8 1,</del>2006.

- 1079 Schorn, S., Ahmerkamp, S., Bullock, E., Weber, M., Lott, C., Liebeke, M., Lavik, G., Kuypers, M. M. M., Graf,
- J. S., and Milucka, J.: Diverse methylotrophic methanogenic archaea cause high methane emissions from
- 1081 seagrass meadows, Proc. Natl. Acad. Sci. U. S. A., 119, e2106628119, doi:10.1073/pnas.2106628119, 2022.
- Schreiber, L., Holler, T., Knittel, K., Meyerdierks, A., and Amann, R.: Identification of the dominant sulfate-
- reducing bacterial partner of anaerobic methanotrophs of the ANME-2 clade: SEEP-SRB1 associated with
- 1084 ANME-2, Environ. Microbiol., 12, 2327–2340, doi:10.1111/j.1462-2920.2010.02275.x, 2010.2010.
- Segarra, K. E. A., Comerford, C., Slaughter, J., and Joye, S. B.: Impact of electron acceptor availability on the
- anaerobic oxidation of methane in coastal freshwater and brackish wetland sediments, Geochim. Cosmochim.
- 1087 Acta, 115, 15–30<del>, doi:10.1016/j.gca.2013.03.029</del>, 2013.
- Sela-Adler, M., Ronen, Z., Herut, B., Antler, G., Vigderovich, H., Eckert, W., and Sivan, O.: Co-existence of
- Methanogenesis and Sulfate Reduction with Common Substrates in Sulfate-Rich Estuarine Sediments, Front.
- 1090 Microbiol., 8, 00766, doi:10.3389/fmicb.2017.00766, 2017.
- Senior, E., Lindström, E. B., Banat, I. M., and Nedwell, D. B.: Sulfate reduction and methanogenesis in the
- sediment of a saltmarsh on the East coast of the United kingdom, Appl. Environ. Microbiol., 43, 987–996,
- 1093 doi:10.1128/aem.43.5.987-996.1982, 1982.1982.
- Seyfferth, A. L., Bothfeld, F., Vargas, R., Stuckey, J. W., Wang, J., Kearns, K., Michael, H. A., Guimond, J., Yu,
- 1095 X., and Sparks, D. L.: Spatial and temporal heterogeneity of geochemical controls on carbon cycling in a tidal
- salt marsh, Geochim. Cosmochim. Acta, 282, 1–18, doi:10.1016/j.gca.2020.05.013, 2020.
- Seymour, C. O., Palmer, M., Becraft, E. D., Stepanauskas, R., Friel, A. D., Schulz, F., Woyke, T., Eloe-Fadrosh,
- 1098 E., Lai, D., Jiao, J.-Y., Hua, Z.-S., Liu, L., Lian, Z.-H., Li, W.-J., Chuvochina, M., Finley, B. K., Koch, B. J.,
- Schwartz, E., Dijkstra, P., Moser, D. P., Hungate, B. A., and Hedlund, B. P.: Hyperactive nanobacteria with host-
- dependent traits pervade Omnitrophota, Nat. Microbiol., 8, 727–744, doi:10.1038/s41564-022-01319-1, 2023.
- 1101 Simmons, S. L. and Edwards, K. J.: Geobiology of Magnetotactic Bacteria, in: Magnetoreception and
- Magnetosomes in Bacteria, edited by: Schüler, D., Springer Berlin Heidelberg, Berlin, Heidelberg, 77–102,
- 1|103 doi:10.1007/7171 039, 2007a.
- 1104 Simmons, S. L. and Edwards, K. J.: Unexpected diversity in populations of the many-celled magnetotactic
- l o prokaryote, Environ. Microbiol., 9, 206–215, doi:10.1111/j.1462-2920.2006.01129.x, 2007b.
- Simmons, S. L., Sievert, S. M., Frankel, R. B., Bazylinski, D. A., and Edwards, K. J.: Spatiotemporal distribution
- of marine magnetotactic bacteria in a seasonally stratified coastal salt pond, Appl. Environ. Microbiol., 70, 6230–
- 1 1 1 0 8 6 2 3 9, doi:10.1128/AEM.70.10.6230 6 2 3 9.2004, 2004. 2004.
- Singh, N., Kendall, M. M., Liu, Y., and Boone, D. R.: Isolation and characterization of methylotrophic
- methanogens from anoxic marine sediments in Skan Bay, Alaska: description of Methanococcoides alaskense sp.
- nov., and emended description of Methanosarcina baltica, Int. J. Syst. Evol. Microbiol., 55, 2531–2538,
- 1|112 doi:10.1099/ijs.0.63886 0, 2005.
- 1113 Sivan, O., Shusta, S. S., and Valentine, D. L.: Methanogens rapidly transition from methane production to iron
- 1 1 14 reduction, Geobiology, 14, 190–203, doi:10.1111/gbi.12172, 2016.

- 1115 Skennerton, C. T., Chourey, K., Iyer, R., Hettich, R. L., Tyson, G. W., and Orphan, V. J.: Methane-fueled
- syntrophy through extracellular electron transfer: Uncovering the genomic traits conserved within diverse
- bacterial partners of anaerobic methanotrophic Archaea, MBio, 8, <a href="https://doi-.org/10.1128/mBio.00530-17">https://doi-.org/10.1128/mBio.00530-17</a>, 2017.
- 1118 Smith, S. J., Page, K., Kim, H., Campbell, B. J., Boerio-Goates, J., and Woodfield, B. F.: Novel synthesis and
- 1 structural analysis of ferrihydrite, Inorg. Chem., 51, 6421–6424, doi:10.1021/ie300937f, 2012.
- 1 20 Sørensen, J. and Glob, E.: Infuence of benthic fauna on trimethylamine concentrations in coastal marine sediments, Mar. Ecol.
- 1 21 Prog. Ser., 39, 15 21, doi:10.3354/meps039015, 1987.
- Sparks, N. H. C., Lloyd, J., and Board, R. G: Saltmarsh ponds—a preferred habitat for magnetotactic bacteria?,
- 1 Lett. Appl. Microbiol., 8, 109–111, doi:10.1111/j.1472-765X.1989.tb00235.x, 1989.1989.
- Stams, A. J. M., Teusink, B., and Sousa, D. Z.: Ecophysiology of Acetoclastic Methanogens, in: Biogenesis of
- 1 | 125 Hydrocarbons, Springer International Publishing, Cham, 109–121, doi:10.1007/978 3 319 78108 2\_21, 2019.
- Stookey, L. L.: Ferrozine---a new spectrophotometric reagent for iron, Anal. Chem., 42, 779–781,
- 1 1 27 doi:10.1021/ac60289a016, 1970.
- 1 Summons, R. E., Franzmann, P. D., and Nichols, P. D.: Carbon isotopic fractionation associated with
- 1 129 methylotrophic methanogenesis, Org. Geochem., 28, 465–475, 1998.
- Sundby, B.: Transient state diagenesis in continental margin muds, Mar. Chem., 102, 2–12,
- 1|131 doi:10.1016/j.marchem.2005.09.016, 2006.
- Sun, L., Toyonaga, M., Ohashi, A., Tourlousse, D. M., Matsuura, N., Meng, X.-Y., Tamaki, H., Hanada, S., Cruz,
- 1133 R., Yamaguchi, T., and Sekiguchi, Y.: Lentimicrobium saccharophilum gen. nov., sp. nov., a strictly anaerobic
- bacterium representing a new family in the phylum Bacteroidetes, and proposal of Lentimicrobiaceae fam. nov,
- Int. J. Syst. Evol. Microbiol., 66, 2635–2642, doi:10.1099/ijsem.0.001103, 2016.
- Suzuki, R., Terada, Y., and Shimodaira, H.: pvclust: An R package for hierarchical clustering with p-values,
- 1137 Github, 2019.
- Tadley, P., Bennett, A., Hansen, K., Hanson, T., Colosi, J., and Goudsouzian, L. K.: Identification of Bacterial
- Taxa Present in a Concrete Pennsylvania Bridge, Microbiol Resour Announc, 12, e0021123,
- 1|140 doi:10.1128/mra.00211-23, 2023.
- 1|142 Solutions synthetic solutions and (Pore)Waterspore)waters: Voltammetric Eevidence of an Aging Processaging
- 1 | 143 process, Environ. Sci. Technol., 34, 2169–2177, doi:10.1021/es990120a, 2000.
- 1144 Taillefert, M., Rozan, T. F., Glazer, B. T., Herszage, J., Trouwborst, R. E., and Luther, G. W., Iii: Seasonal Variations of
- 1 45 Soluble Organic Fe(III) in Sediment Porewaters as Revealed by Voltammetric Microelectrodes, in: Environmental
- 1 146 Electrochemistry, vol. 811, American Chemical Society, 247 264, doi:10.1021/bk 2002 0811.ch013, 2002a.
- 1 147 Taillefert, M., Hover, V. C., Rozan, T. F., Theberge, S. M., and Luther, G. W.: The influence of sulfides on soluble organic
- 1 1 1 48 Fe(III) in anoxic sediment porewaters, Estuaries, 25, 1088–1096, doi:10.1007/BF02692206, 2002b.

- Taillefert, M., Neuhuber, S., and Bristow, G.: The effect of tidal forcing on biogeochemical processes in intertidal
- salt marsh sediments, Geochem. Trans., 8, 6, doi:10.1186/1467-4866-8-6, 2007.
- Tang, J., Zhuang, L., Ma, J., Tang, Z., Yu, Z., and Zhou, S.: Secondary mineralization of ferrihydrite affects
- microbial methanogenesis in Geobacter-Methanosarcina cocultures, Appl. Environ. Microbiol., 82, 5869–5877,
- 1|153 doi:10.1128/AEM.01517-16, 2016.
- Waite, T. J., Kraiya, C., Trouwborst, R. E., Ma, S., and Luther, G. W., III: An investigation into the suitability of
- bismuth as an alternative to gold-amalgam as a working electrode for the in situ determination of chemical redox
- 1 | 156 species in the natural environment, Electroanalysis, 18, 1167–1172, doi:10.1002/elan.200603519, 2006.
- Wang, H., Byrne, J. M., Liu, P., Liu, J., Dong, X., and Lu, Y.: Redox cycling of Fe(II) and Fe(III) in magnetite
- 1|158 accelerates aceticlastic methanogenesis by Methanosarcina mazei, Environ. Microbiol. Rep., 12, 97–109,
- 1|159 doi:10.1111/1758-2229.12819, 2020.
- Wang, J., Zheng, Q., Wang, S., Zeng, J., Yuan, Q., Zhong, Y., Jiang, L., and Shao, Z.: Characterization of two
- novel chemolithoautotrophic bacteria of Sulfurovum from marine coastal environments and further comparative
- genomic analyses revealed species differentiation among deep-sea hydrothermal vent and non-vent origins, Front.
- Wang, X.-C. and Lee, C.: Sources and distribution of aliphatic amines in salt marsh sediment, Org. Geochem.,
- 1 1 1 6 5 22, 1005 1021, 1994a.
- Wang, X.-C. and Lee, C.: Sources and distribution of aliphatic amines in salt marsh sediment, Org. Geochem.,
- 1 1 22, 1005–1021, doi:10.1016/0146-6380(94)90034-5, 1994 1994b.
- Watkins, A. J., Roussel, E. G., Parkes, R. J., and Sass, H.: Glycine betaine as a direct substrate for methanogens
- l|169 (Methanococcoides spp.), Appl. Environ. Microbiol., 80, 289–293, doi:10.1128/AEM.03076-13, 2014.
- Winfrey, M. R. and Ward, D. M.: Substrates for sulfate reduction and methane production in intertidal sediments,
- 1 | 171 Appl. Environ. Microbiol., 45, 193–199, doi:10.1128/aem.45.1.193-199.1983, 1983.1983.
- 1172 Xiao, K.-O., Beulig, F., Kjeldsen, K. U., Jørgensen, B. B., and Risgaard-Petersen, N.: Concurrent methane
- production and oxidation in surface sediment from Aarhus Bay, Denmark, Front. Microbiol., 8, 1198,
- 1174 doi:10.3389/fmicb.2017.01198, 2017.
- 1175 Xiao, K. Q., Beulig, F., Røy, H., Jørgensen, B. B., and Risgaard-Petersen, N.: Methylotrophic methanogenesis
- fuels cryptic methane cycling in marine surface sediment, Limnol. Oceanogr., 63, 1519–1527,
- 1|177 doi:10.1002/LNO.10788, 2018.
- 1178 Xiao, L., Lichtfouse, E., and Senthil Kumar, P.: Advantage of conductive materials on interspecies electron
- 1179 transfer-independent acetoclastic methanogenesis: A critical review, Fuel, (Lond.), 305, 121577.
- 1|180 doi:10.1016/j.fuel.2021.121577, 2021.
- 1181 Xue, P., Chang, L., Pei, Z., and Harrison, R. J.: The origin of magnetofossil coercivity components: Constraints
- from coupled experimental observations and micromagnetic calculations, J. Geophys. Res. Solid Earth, 129,
- 1|183 <u>e2023JB028501</u>, https://doi<sub>:.</sub>org/10.1029/2023jb028501, 2024.

- 1184 Xu, H., Chang, J., Wang, H., Liu, Y., Zhang, X., Liang, P., and Huang, X.: Enhancing direct interspecies electron
- transfer in syntrophic-methanogenic associations with (semi)conductive iron oxides: Effects and mechanisms,
- 1 | 186 Sci. Total Environ., 695, 133876, doi:10.1016/j.scitotenv.2019.133876, 2019.2019.
- 1 Yang, X-H., Scranton, M. I., and Lee, C.: Seasonal variations in concentration and microbial uptake of
- 1 methylamines in estuarine waters, Mar. Ecol. Prog. Ser., Marine Ecology Progress Series, 108, 303–312,
- 1 189 doi:10.3354/meps108303, 1994.
- Yee, M. O. and Rotaru, A.-E.: Extracellular electron uptake in Methanosarcinales is independent of multiheme c-
- 1|191 type cytochromes, Sci. Rep., 10, 372, doi:10.1038/s41598-019-57206-z, 2020.
- Yuan, J., Ding, W., Liu, D., Xiang, J., and Lin, Y.: Methane production potential and methanogenic archaea
- 1193 community dynamics along the Spartina alterniflora invasion chronosequence in a coastal salt marsh, Appl.
- 1|194 Microbiol. Biotechnol., 98, 1817–1829, doi:10.1007/s00253-013-5104-6, 2014.
- Yuan, J., Ding, W., Liu, D., Kang, H., Xiang, J., and Lin, Y.: Shifts in methanogen community structure and
- function across a coastal marsh transect: effects of exotic Spartina alterniflora invasion, Sci. Rep., 6, 18777,
- 1|197 doi:10.1038/srep18777, 2016.
- Yuan, J., Liu, D., Ji, Y., Xiang, J., Lin, Y., Wu, M., and Ding, W.: Spartina alterniflora invasion drastically
- increases methane production potential by shifting methanogenesis from hydrogenotrophic to methylotrophic
- 1200 pathway in a coastal marsh, J. Ecol., 107, 2436–2450, doi:10.1111/1365.2745.13164, 2019.
- Yuan, T., Ko, J. H., Zhou, L., Gao, X., Liu, Y., Shi, X., and Xu, Q.: Iron oxide alleviates acids stress by
- facilitating syntrophic metabolism between Syntrophomonas and methanogens, Chemosphere, 247, 125866,
- 1203 doi:10.1016/j.chemosphere.2020.125866, 2020.2020.
- Yu, L., He, D., Yang, L., Rensing, C., Zeng, R. J., and Zhou, S.: Anaerobic methane oxidation coupled to
- ferrihydrite reduction by Methanosarcina barkeri, Sci. Total Environ., 844, 157235,
- 1206 doi:10.1016/j.scitotenv.2022.157235, 2022.
- 1207 Zachara, J. M., Kukkadapu, R. K., Fredrickson, J. K., Gorby, Y. A., and Smith, S. C.: Biomineralization of
- poorly crystalline Fe(III) oxides by dissimilatory metal reducing bacteria (DMRB), Geomicrobiol. J., 19, 179–
- 1209 207<del>, doi:10.1080/01490450252864271</del>, 2002.
- 1210 Zhang, Z., Zimmermann, N. E., Stenke, A., Li, X., Hodson, E. L., Zhu, G., Huang, C., and Poulter, B.: Emerging
- role of wetland methane emissions in driving 21st century climate change, Proc. Natl. Acad. Sci. U. S. A., 114,
- 1212 9647–9652<del>, doi:10.1073/pnas.1618765114</del>, 2017.
- Zhao, N., Ding, H., Zhou, X., Guillemot, T., Zhang, Z., Zhou, N., and Wang, H.: Dissimilatory iron-reducing
- 1214 microorganisms: The phylogeny, physiology, applications and outlook, Crit. Rev. Environ. Sci. Technol., 1-26,
- 1215 doi:10.1080/10643389.2024.2382498, 202455, 73–98, 2025.
- 1216 Zhao, Z., Li, Y., Yu, Q., and Zhang, Y.: Ferroferric oxide triggered possible direct interspecies electron transfer
- between Syntrophomonas and Methanosaeta to enhance waste activated sludge anaerobic digestion, Bioresour.
- 1218 Technol., 250, 79–85, doi:10.1016/j.biortech.2017.11.003, 2018.

- 1219 Zhao, Z., Sun, C., Li, Y., Peng, H., and Zhang, Y.: Upgrading current method of anaerobic co-digestion of waste
- activated sludge for high-efficiency methanogenesis: Establishing direct interspecies electron transfer via
- 1221 ethanol-type fermentation, Renew. Energy, 148, 523–533, doi:10.1016/j.renene.2019.10.058, 2020.
- Zheng, S., Liu, F., Wang, B., Zhang, Y., and Lovley, D. R.: Methanobacterium capable of direct interspecies
- l223 electron transfer, Environ. Sci. Technol., 54, 15347–15354, doi:10.1021/acs.est.0c05525, 2020.
- Zheng, S., Li, M., Liu, Y., and Liu, F.: Desulfovibrio feeding Methanobacterium with electrons in conductive
- methanogenic aggregates from coastal zones, Water Res., 202, 117490, doi:10.1016/j.watres.2021.117490, 2021.
- 1226 Zhou, S., Xu, J., Yang, G., and Zhuang, L.: Methanogenesis affected by the co-occurrence of iron(III) oxides and
- 1227 humic substances, FEMS Microbiol. Ecol., 88, 107–120, doi:10.1111/1574\_6941.12274, 2014.
- Zhou, Z., Pan, J., Wang, F., Gu, J.-D., and Li, M.: Bathyarchaeota: globally distributed metabolic generalists in
- 1229 anoxic environments, FEMS Microbiol. Rev., 42, 639–655, doi:10.1093/femsre/fuy023, 2018.
- Zhuang, L., Xu, J., Tang, J., and Zhou, S.: Effect of ferrihydrite biomineralization on methanogenesis in an
- anaerobic incubation from paddy soil, J. Geophys. Res. Biogeosci., 120, 876–886, doi:10.1002/2014jg002893,
- 1232 2015.

1236

- Zhuang, L., Tang, Z., Yu, Z., Li, J., and Tang, J.: Methanogenic Activity and Microbial Community Structure in
- Response to Different Mineralization Pathways of Ferrihydrite in Paddy Soil, Front Earth Sci., 7, 00325,
- 1235 doi:10.3389/feart.2019.00325, 2019.